Journal of Controlled Release 328 (2020) 470–489

Contents lists available at ScienceDirect

Journal of Controlled Release

journal homepage: www.elsevier.com/locate/jconrel

Review article

$CaCO_3$ crystals as versatile carriers for controlled delivery of antimicrobials

Ana M. Ferreira[a], Anna S. Vikulina[b], Dmitry Volodkin[a,*]

[a] School of Science and Technology, Department of Chemistry and Forensics, Nottingham Trent University, Clifton Lane, Nottingham NG11 8NS, UK
[b] Fraunhofer Institute for Cell Therapy and Immunology, Branch Bioanalytics and Bioprocesses, Am Muhlenberg 13, Potsdam, Golm 14476, Germany

ARTICLE INFO

Keywords:
Calcium carbonate
Drug delivery carriers
Vaterite
Calcite
Aragonite
Antimicrobial resistance

ABSTRACT

$CaCO_3$ crystals have been known for a long time as naturally derived and simply fabricated nano(micro)-sized materials able to effectively host and release various molecules. This review summarises the use of $CaCO_3$ crystals as versatile carriers to host, protect and release antimicrobials, offering a strong tool to tackle antimicrobial resistance, a serious global health problem. The main methods for the synthesis of $CaCO_3$ crystals with different properties, as well as the approaches for the loading and release of antimicrobials are presented. Finally, prospects to utilize the crystals in order to improve the therapeutic outcome and combat antimicrobial resistance are highlighted. Ultimately, this review intends to provide an in-depth overview of the application of $CaCO_3$ crystals for the smart and controlled delivery of antimicrobial agents and aims at identifying the advantages and drawbacks as well as guiding future works, research directions and industrial applications.

1. Introduction

The discovery of the first antibiotics marked a turning point in the history of medicine. The prospects of cure for patients with bacterial infections changed radically for the best. However, antimicrobials heavy and sometimes incorrect use promoted the appearance of alarming levels of resistance. Antibiotic-resistant infections cause per year at least 25,000 deaths in the European Union [1] and 35,000 in the United States of America [2], with the prospects of causing 10 million deaths globally per year by 2050 if nothing is done to address the problem [3]. The lack of new classes of antibiotics in the market, and the lower interest of pharmaceutical companies in developing new drugs (low success and profits) accentuates the severity of the problem [4–6].

The rational use of antibiotics is essential to tackle the levels of bacterial resistance. Numerous campaigns and discussion groups have been created to raise the attention of healthcare practitioners and the general public, nonetheless there is still a long way to go.

Drug delivery systems are extremely important to improve the pharmacokinetics of antimicrobials, antimicrobial activity, patients' adherence to treatment programs, decrease side effects, and supress the appearance of new resistance mechanisms [7–10].

The antibiotics used clinically today present some drawbacks such as limited stability (due to variation of temperature and pH, presence of chelating agents), solubility, bioavailability, distribution/penetration in the target tissue, and short half-lifes [6,8,11]. Moreover, new therapeutic agents, *e.g.* antimicrobial peptides, are sensitive to enzymatic decomposition [12].

In an attempt to improve drug delivery effectiveness and the chemotherapeutic outcomes, new carriers have been developed to effectively deliver antimicrobials. These include mesoporous silica, liposomes, quantum dots, dendrimers, solid lipid nanoparticles, nano- and micro-emulsions, gels, carbon nanomaterials, magnetic nanoparticles, microneedles and polymeric microparticles [13–17]. The popular polymer-based carriers are typically made of polymers such as chitosan, alginate, gelatin, albumin, collagen, poly(vinyl pyrrolidone), poly(acrylic acid), poly(vinyl alcohol), poly(methyl methacrylate), polyurethanes, polystyrene, poly(lactic-co-glycolic) acid, poly(lactic acid) and polyglycolic acid, with the last three being the most studied [16–19]. Some of the delivery carriers enumerated are already used in commercialized products [18,19]. However, the often intricate and multi-step production, cytotoxicity, recognition by the immune system, and significant loss of bioactivity in the complex biological media retards their further clinical translation and urges the search for alternative carriers that can bypass these limitations [13,20].

$CaCO_3$ is a versatile mineral with different applications such as construction (limestone), bone cements, dental implants, scaffolds, filler for paints, coatings, paper, pigments and plastics [21–24]. $CaCO_3$ is also included in different pharmacopoeias and is widely commercialized for pharmaceutical use in oral formulations as an excipient/active substance (antacids and medicines for the treatment of calcium deficiency). More recently it has been employed as a vector for drug

* Corresponding author.
E-mail address: dmitry.volodkin@ntu.ac.uk (D. Volodkin).

https://doi.org/10.1016/j.jconrel.2020.08.061
Received 2 July 2020; Received in revised form 27 August 2020; Accepted 28 August 2020
Available online 05 September 2020

delivery and as a decomposable template for assembly of multilayer capsules [21,22,25,26]. $CaCO_3$ availability, low price, biocompatibility, biodegradability, high surface area, simple synthesis, tuneable and stimuli-responsive properties, make it an excellent candidate for loading and controlled release of various drugs [27]. Importantly, the use of calcium carbonate as a food and pharmaceutical additive/ingredient is approved by the Food and Drug Administration Agency (FDA). Recently, the European Food Safety Agency Panel on Food Additives and Nutrient Sources added to Food, re-evaluated its usage taking into account the latest available toxicological data and confirmed no toxicological concerns for the use of $CaCO_3$ [28]. Numerous works have reported the use of $CaCO_3$, mainly the vaterite polymorph, for biomedical applications, *e.g.*, for encapsulation of enzymes, hormones, DNA, growth factors, and drugs [21,29–41]. The employment $CaCO_3$ crystals as carriers for delivery of antimicrobials was demonstrated for the first time about 16 years ago and was followed by several scientific reports demonstrating the advantages of $CaCO_3$ crystals for antimicrobials delivery over other drug delivery systems. $CaCO_3$ protects the antimicrobial agents from the external environment and can be designed to release the cargo in a controlled way and on demand. One of the most interesting characteristics of the $CaCO_3$ crystals is their sensitivity to different pH values which allows the cargo to be released on specific sites or conditions without affecting the antimicrobial activity. Moreover, the easily adjustable properties of $CaCO_3$ crystals (size, solubility, shape, composition) makes them attractive and dynamic drug delivery systems for different targets, microenvironment conditions and routes of administration.

This review summarises the use of $CaCO_3$ nano- and micro-crystals as versatile carriers to deliver antimicrobials in a controlled and programmed manner as highly desired for multiple drug delivery applications. The first part of this review intends to look at the main synthesis routes of $CaCO_3$ crystals and the factors that affect the crystal properties (*e.g.* size, morphology, structure) and can be used to fine tune $CaCO_3$ crystals properties. In the second part, the approaches for loading/release of antimicrobials into/from the crystals and the antimicrobial performance of $CaCO_3$ crystals are addressed. In the end of the review, the outlooks for better therapeutic outcome and effective tackling of the antimicrobial resistance using $CaCO_3$ crystals are given (Fig. 1).

2. $CaCO_3$ crystals

$CaCO_3$ is a mineral that occurs in three anhydrous crystalline forms (aragonite, vaterite and calcite) and two hydrated crystalline forms with limited occurrence, *i.e.*, ikaite and monohydrocalcite [42,43]. $CaCO_3$ can also occur as amorphous $CaCO_3$ (ACC), which is highly unstable and rapidly transforms into the metastable or stable polymorphs. Calcite is the most thermodynamically stable polymorph at standard conditions, and like the other anhydrous polymorphs, ACC precedes its formation [43,44].

Each $CaCO_3$ anhydrous polymorph has a typical morphology. Aragonite presents a needle-like shape, while vaterite and calcite have a spherical and rhombohedral morphology, respectively (Fig. 2) [45]. Nonetheless, this shape can be changed by altering different synthesis conditions [22].

Bare vaterite crystals are unstable in aqueous solutions recrystallizing to calcite within some hours or a few days; this can, however, be affected by the presence of additives like nanoparticles and different types of polymers [21,22,48,49]. Despite this, its porous structure, high surface area, tunable morphology, size (which can range from tens of nanometres to tens of micrometres) and recrystallization kinetic, makes it an attractive drug carrier [21,50]. From all the $CaCO_3$ polymorphs vaterite presents the best properties for drug delivery, nonetheless, being a metastable phase between ACC and calcite, it poses some challenges and opportunities. These are related to keeping vaterite stable and maintaining its porous structure, but also using vaterite "limitations" as triggers for drug delivery, *i.e.* recrystallization to calcite and pH sensitivity.

2.1. Main routes of $CaCO_3$ synthesis

There are four main $CaCO_3$ synthesis methods: CO_2 bubbling, slow carbonation, reverse emulsion and solution precipitation (Fig. 3) [51,52]. CO_2 bubbling or carbonation is the main industrial method and consists of bubbling CO_2 in a $Ca(OH)_2$ solution (Eq. (3) and Eq. (4)) obtained from limestone calcination (Eq. (1)) followed by hydration (Eq. (2)) [53–55]. This method results mainly in nano-sized calcite crystals [22,56], nonetheless the size, polymorph type, morphology and properties of the formed particles can be controlled by adding additives, changing the Ca^{2+} concentration, or the operating conditions such as liquid or gas flow rate, CO_2 pressure and temperature [22].

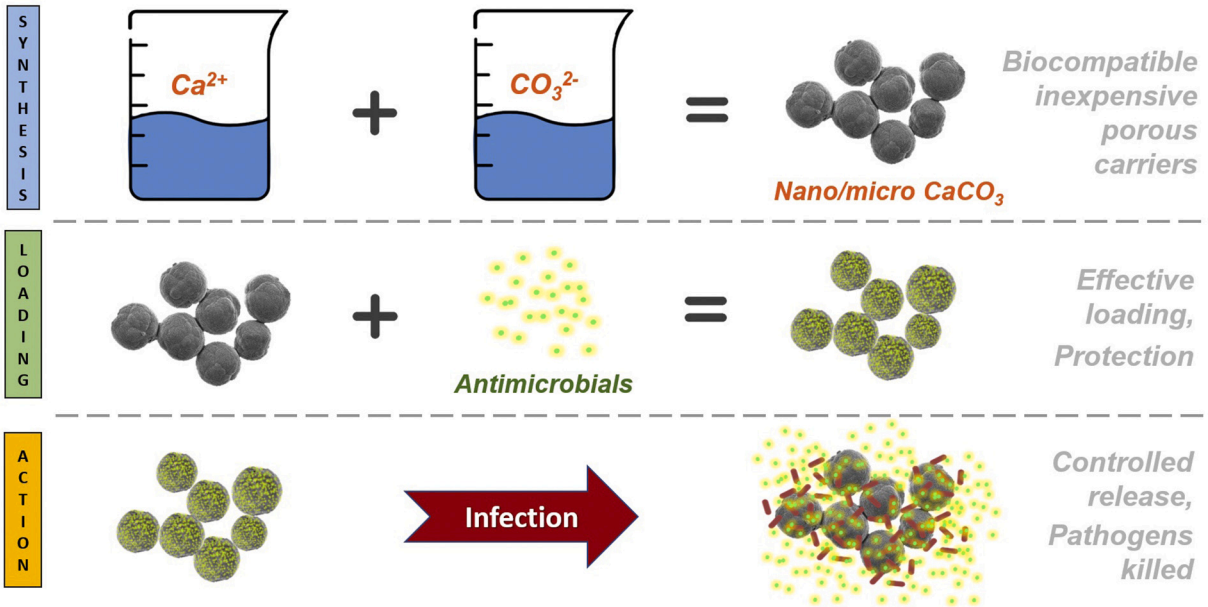

Fig. 1. Outline of the main topics covered in this review.

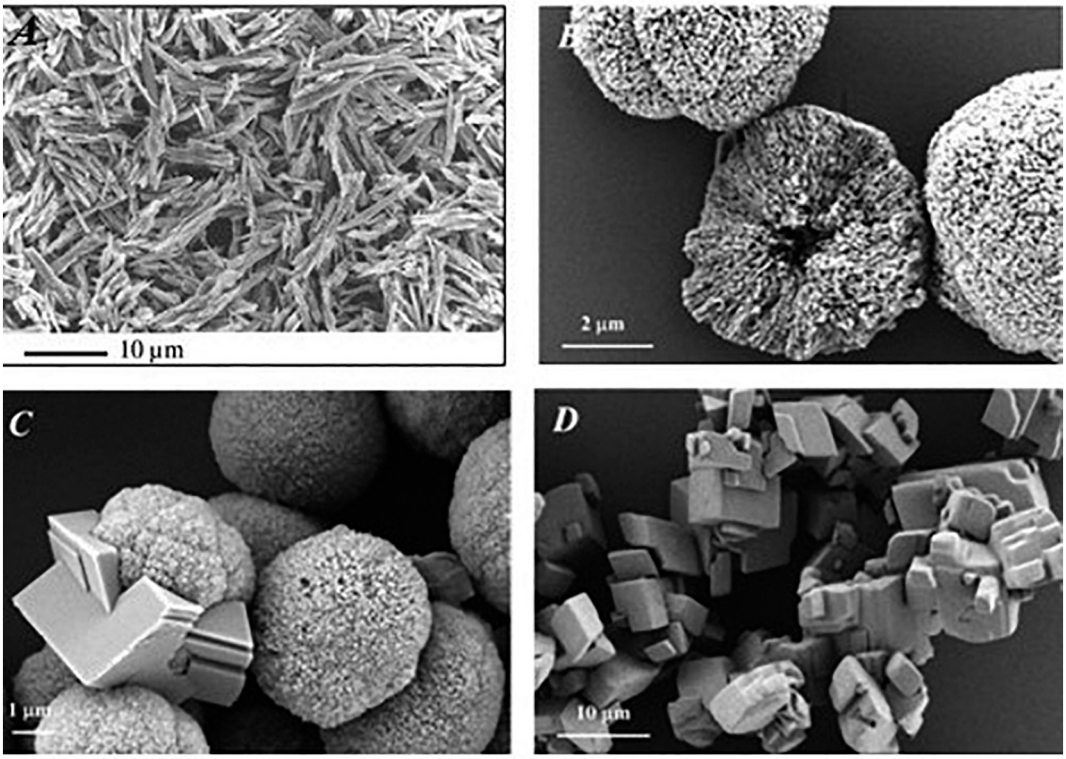

Fig. 2. SEM images of aragonite (A), broken vaterite (B), vaterite and vaterite recrystallizing to calcite (C) and calcite (D). Image A adapted from Lucas et al. [46] and Images B, C, D from Volodkin D. et al. [47]. Copyright 2001,with permissions from Elsevier (Image A) and Copyright 2004, with permission from American Chemical Society (Image B, C and D).

$$CaCO_3(\text{limestone}) \rightleftharpoons CaO + CO_2\ T{\sim}900°C \quad (1)$$

$$CaO + H_2O \rightleftharpoons Ca(OH)_2 \quad (2)$$

$$CO_2 + H_2O \rightleftharpoons H_2CO_3 \quad (3)$$

$$H_2CO_3 + Ca(OH)_2 \rightleftharpoons CaCO_3(\text{crystals}) + 2H_2O \quad (4)$$

Slow carbonation reaction is another carbonation method which is less applied. It consists of the production of carbonate ions through the dissolution of CO_2 resultant from the slow hydrolysis of dimethyl carbonate, ammonium carbonate, or other compounds (Eq. (5)), under alkaline conditions [22,57–59].

$$(NH_4)_2CO_3 \rightleftharpoons 2NH_3 + CO_2 + H_2O \quad (5)$$

Reverse emulsion (water in oil or W/O) synthesis comprises a system composed of a hydrophobic continuous phase with dispersed hydrophilic droplets (CO_3^{2-} or Ca^{2+} solutions) stabilized by a surfactant. $CaCO_3$ is formed when the emulsions are mixed, and the micelles containing CO_3^{2-} and Ca^{2+} ions collide, forming "micro-reactors". This method allows the synthesis of nano- and micro-particles with narrow size distributions. The type of $CaCO_3$ polymorph, size and morphology

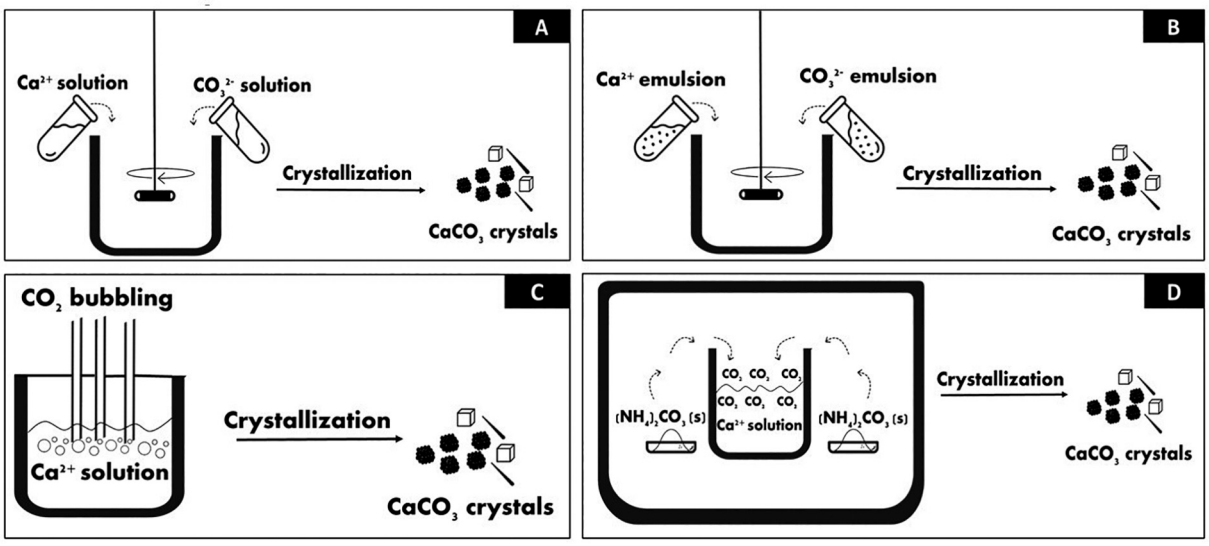

Fig. 3. Main $CaCO_3$ synthesis methods: (a) solution precipitation method; (b) reverse emulsion (W/O) method; (c) CO_2 bubbling method and (d) slow carbonation method. Figure redrawn based on the work of Boyjoo et al. [22].

of the crystals can be controlled by adding different additives, changing the pH, temperature, reaction time as well as the molar ratios of water to oil, water to surfactant, and Ca^{2+} to CO_3^{2-} [22,60].

The solution route, also known as solution precipitation method or mixing method [61], is the main method used on a lab-scale, and comprises the mixing of supersaturated solutions of CO_3^{2-} and Ca^{2+} containing salts with or without additives. It is the simplest and quickest method, when compared with the carbonation or reverse emulsion, and the modification of different synthesis variables allows to adjust the size, shape, and type of polymorph synthetized. Up to the best of our knowledge, nowadays, only this method has been up scaled for commercial fabrication of vaterite microcrystals (*e.g.* PlasmaChem GmbH, Germany). In relation to the encapsulation of antimicrobials, the solution precipitation method has received the most widespread use up to now.

2.2. Synthesis conditions effect on $CaCO_3$ crystals

Various synthesis conditions like presence of additives, solvent type, pH, rate and mode of component mixing, temperature and precursor concentrations can significantly affect the properties of the crystals. Notably, the effect of most of these synthesis conditions, like pH, supersaturation, temperature, mixing mode and solvents, are transversal to the majority of the synthesis/loading methods. Most of these variables have been extensively studied, and the best conditions to produce crystals with specific size, polymorph form, or other required properties have been determined. In the sections below, the effect of these variables will be addressed in more detail, with a special focus on the solution precipitation method, due to its widespread use and the high number of detailed studies.

2.2.1. pH

The main effect of pH is on the availability of carbonate ions. At pH ≤ 8, carbonate ions are mainly protonated to bicarbonate, decreasing CO_3^{2-} concentration, and consequently interfering with the precipitation of $CaCO_3$. Therefore, pH values above 8 are necessary for $CaCO_3$ synthesis. However, within the basic pH range, very high pH values create high nucleation rates, promoting uncontrolled crystal growth and the formation of large and irregular crystals [22].

The pH value also governs the effect of some additives, mainly when they possess ionizable groups, *e.g.*, carboxyl group which is ionized at basic pH and originates sites able to interact with Ca^{2+} controlling the formation of the crystals and resulting in particles with a more uniform size distribution [22].

Oral et al. [62] studied the influence of pH on $CaCO_3$ synthesis at room temperature, through the solution precipitation method in the presence of ethylene glycol (EG). The results demonstrated that vaterite particles formed independently of the $[Ca^{2+}]$:$[CO_3^{2-}]$ ratio, when the pH of the precursor solutions was 8 and 10. However, above pH 10, the ratio of the salts started to play a role in the type of polymorph formed. Oral and co-workers verified that the size of $CaCO_3$ particles increased with an increase in the pH of the precursor solutions.

Clifford Y. et al. [63] studied the effect of different synthesis conditions, including pH, on the polymorphism of $CaCO_3$ using a constant-composition method. The experiment comprised mixing solutions of $CaCl_2$ with Na_2CO_3 at constant conditions. The authors demonstrated the effect of pH on the type of polymorph formed and that vaterite is the main polymorph formed between pH 8.5 and 10 at 24 °C.

Han Y. et al. [64] studied the effect of pH on the type of polymorph formed by the carbonation method and, overall, it was also demonstrated that higher pH values resulted in a decrease of the vaterite fraction (Fig. 4) in favour of calcite.

2.2.2. Temperature

Temperature is an important factor when synthesizing $CaCO_3$ crystals, as it influences the polymorphism of the particles produced

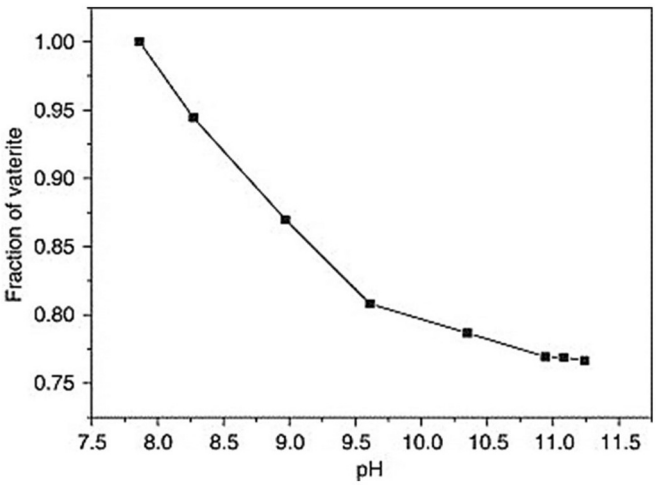

Fig. 4. Fraction of vaterite at different pH values. Synthesis based on passing CO_2/N_2 mixed gas into a $CaCl_2$ solution at 20 °C. Reprinted from Han Y. et al. [64]. Copyright 2006, with permission from Elsevier.

[65]. Ogino et al. [66] synthesized $CaCO_3$ particles by mixing $CaCl_2$ (1.93×10^{-2} M) with Na_2CO_3 (9.26×10^{-3} M) at a molar ratio of 2 to 1, respectively, and studied the effect of temperature on the type of polymorph formed. Ogino T. and co-workers verified that at low temperatures (≤ 20 °C) calcite is the main polymorph formed, while between 30 and 40 °C vaterite is produced at higher contents, and at temperatures around 70 °C aragonite is the predominant polymorph. Similar findings were reported by Chen et al. [67], who synthesized $CaCO_3$ by mixing $CaCl_2$ (0.25 M) and NH_4HCO_3 (0.25 M) (Fig. 5). Nonetheless, in contrast to the work of Ogino et al. [66], the formation of vaterite was also observed at 60 °C. Ševčík R. et al. [68], also reported the synthesis of vaterite at 60 °C by mixing equal molar ratios of $CaCl_2$ (2.0 M) and K_2CO_3 (2.0 M). This difference can be explained by the higher molar ratios used by Ševčík R. et al. [68] and Chen et al. [67]. This demonstrates that the initial concentration of the reagents can modulate the temperature effect on the type of polymorph formed. This effect was previously reported by Ma et al. [65].

Interestingly, the temperature during synthesis of vaterite polymorph affects its mesoporous internal structure. Feoktistova et al. [25], verified that vaterite crystals synthetized without additives at higher temperatures (45 °C) present larger pore size, a propertie that might be crucial for many bio-applications.

2.2.3. Supersaturation and $[Ca^{2+}]$:$[CO_3^{2-}]$ ratio

The concentration of the precursor salts and the $[Ca^{2+}]$:$[CO_3^{2-}]$ ratio affect the synthesis duration, type, and size of the polymorph formed. The crystallization takes place just when the supersaturation is reached. The high supersaturation results in higher nucleation ratios and lower induction times [69]. According to the "Ostwald's step rule" at a low supersaturation the stable polymorph (calcite) may preferentially precipitate while at a high supersaturation the metastable polymorph (vaterite and aragonite) tends to form [70,71]. Kitamura [70] verified this tendency when synthesizing $CaCO_3$ by mixing $CaCl_2$ and Na_2CO_3 solutions at different concentrations at ca 25 °C. It was shown that vaterite tends to precipitate at a high supersaturation (200 mM) while calcite mainly precipitates at a lower concentration (50 mM) [70]. The same trend was verified by Ma et al. [65] and Ogino et al. [66], who reported that the relative abundance of vaterite increased by increasing the concentrations of calcium and carbonate ions at 25 °C. Nonetheless, it has been demonstrated that when the supersaturation of ACC is lower than 1, *i.e.* the ion activity product of the initial supersaturated solution is lower than the solubility product of ACC at 25 °C, only vaterite crystals are formed and present a peculiar

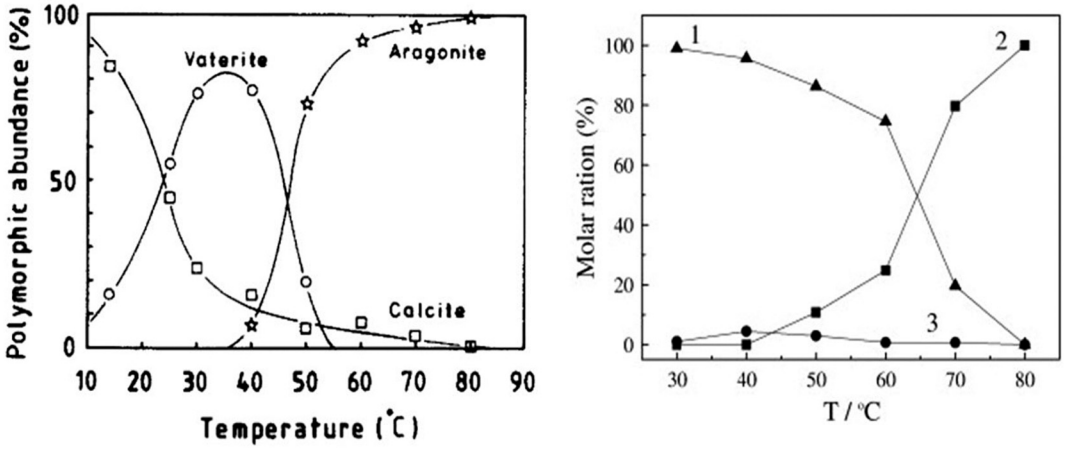

Fig. 5. Polymorphic abundance (%) of crystalline carbonates at the early metastable stages as a function of temperature.1 - vaterite; 2 - aragonite and 3 - calcite. Adapted from Ogino et al. [66] (left) and Chen et al. [67] (right). Copyright 1987 and 2009, respectively, with permission from Elsevier.

hexagonal plate-like shape [66,72]. Moreover, the synthesis of these vaterite crystals implies longer induction times (time needed for the detection of the first newly created particles) due to the low initial concentrations (c_i) of the salts solutions: $c_i(Ca^{2+}) = c_i(CO_3^{2-}) < 1.8$ mM) [72]. The supersaturation rate also influences the size of $CaCO_3$ crystals. Higher supersaturation promotes the formation of smaller crystals due to a higher nucleation rate at the same total mass of the precipitate [50,61,70].

Finally, the ratio of the precursor salt affects mainly the size and shape of the crystals. Nonetheless, at a very high pH value it can also affect the type of polymorph formed [62]. It has been demonstrated that higher concentrations of CO_3^{2-} ions, in comparison with Ca^{2+} ions, result in the formation of crystals with more ellipsoidal geometries while lower concentrations promote the formation of isotropic spherical particles (Fig. 6) [62,73].

2.2.4. Reagent mixing

The reagents mixing order and stirring speed affect mainly the morphology, size and size distribution of the crystals [22]. Volodkin D. et al. [74] tested the effect of the stirring time (15, 20, 30 and 40 s) and speed (400, 650 and 900 rpm) on the synthesis of $CaCO_3$ by the solution route. They concluded that higher stirring times and speeds lead to the formation of more nuclei and, as a result, smaller crystals due to heterogeneous nucleation of the crystal growth. Just by varying the stirring time and speed, the authors were able to synthesize particles with sizes ranging between 3 and 20 μm. Other authors have also reported similar results [41,75].

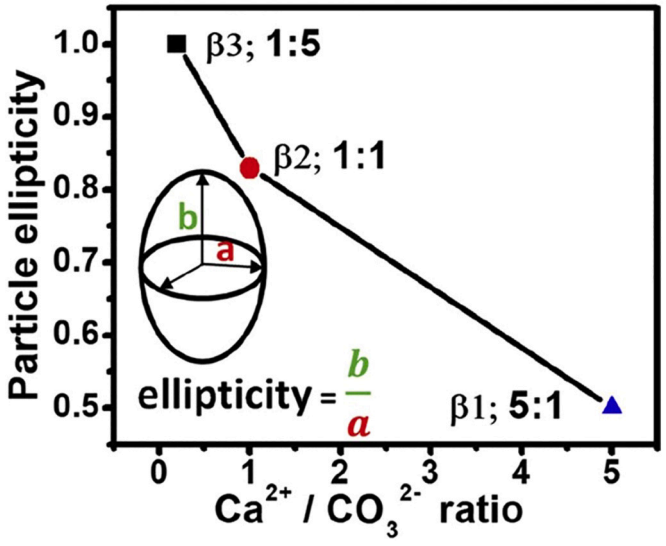

Fig. 6. Dependence of particle ellipticity on the $[Ca^{2+}]$:$[CO_3^{2-}]$ ratio. $CaCO_3$ crystals were synthesized at room temperature by mixing $CaCl_2$ and Na_2CO_3 solutions. Reprinted from Bahrom et al. [73]. Copyright 2019, with permission from American Chemical Society.

Ševčík et al. [68] and Mori et al. [76] verified that when mixing precursor solutions with very high concentrations (1–2 M) the stirring speed is crucial for the type of the polymorph formed. Inadequate stirring creates different local concentrations in the same solution/gel, promoting the formation of calcite. On the other hand, a homogenous and continuous agitation results in the same salts concentration in the bulk and the formation of higher contents of vaterite.

The order of addition of reagents also affects the characteristics of the crystal. Wang et al. [77] demonstrated that adding the CO_3^{2-} ion solution to the Ca^{2+} ion solution (quick mixing or dropwise) results in smaller crystals with a uniform size distribution. However, with the opposite addition, the crystals become larger and have a non-uniform size distribution. This effect is more pronounced when the Ca^{2+} solution is added dropwise to the CO_3^{2-} solution. The different results are related to the different pH values of the precursor solutions [77,78]. When Ca^{2+} containing salts solutions (pH ≈ 6.41 to 8.83 for $CaCl_2$ solutions with a concentration between 2 mM to 800 mM at 25 °C [65]) are added to CO_3^{2-} containing salts solutions (pH ≈ 11.0 for Na_2CO_3 solutions with a concentration between 2 mM and 800 mM at 25 °C [65]) the transitory initial pH value, before reaching the equilibrium, is higher than when the opposite addition is done. This results in high nucleation rates with uncontrolled crystal growth and formation of large crystals with inhomogeneous size distribution [22,77].

2.2.5. Solvent

Water is the primordial, most used, and well-studied solvent for the synthesis of $CaCO_3$. Nonetheless, mixtures of water with other solvents have also been used to form $CaCO_3$ crystals [45,48,73,79,80]. These solvents include ethanol, propranolol, methanol, polyethylene glycol (PEG), glycerine, *N*,*N*-dimethylformamide and EG [45,48,73,79–81]. Overall, the solvents decrease the solubility of $CaCO_3$ which results in higher supersaturation ratios and the formation of smaller particles. Some of these solvents like PEG, glycerine and EG also increase the density of the reaction media which diminishes the molecular diffusion and reduces the crystal growth rate and the probability of nucleation [73,79]. Moreover, low or no water content results in the stabilization of $CaCO_3$ particles formed at the early stages of the synthesis [73].

Solvents can also affect the type of polymorph formed. Sand K. et al. [45] demonstrated that the combination of water (50%) with ethanol (50%) promotes the formation of aragonite at 24 °C, which usually just

occurs at high temperatures in aqueous solutions.

2.2.6. Additives

Numerous articles have reported the effect of additives on the properties of $CaCO_3$ crystals. Nonetheless, additives use is mainly empirical due to their multiple roles that can be difficult to define. Moreover, the effect of additives on the properties of the crystals can depend on the additive concentration and other experimental conditions [82].

The type of additives tested on $CaCO_3$ synthesis include surfactants, synthetic polymers, biomolecules, biopolymers, and inorganic compounds. These compounds affect the crystallization process (cluster formation, prenucleation, nucleation, and growth), recrystallization kinetics, and can promote the formation of one polymorph form over the others. Moreover, it can lead to the formation of crystals with different sizes and shapes (flower, peanut, pyramid-like *etc.*) [21,22,82,83]. The incorporation of additives tries, to some extent, mimic the capacity of different organisms to build and control the formation of different $CaCO_3$ structures by combining it with organic or inorganic compounds (biomineralization) [22,84].

Reviews summarizing the effects of additives on the synthesis and stabilization of $CaCO_3$ can be found elsewhere [21,22,48]. Despite the large number of variables when studying the effect of additives, it has been reported that synthetic polymers, at the right concentration, usually induce the formation of vaterite spheres with a uniform size distribution. Polyacrylic acid (PAA) and polystyrene sulfonate (PSS) are reported as the most effective polymers in the retention of vaterite spherical shape [22,48]. Biopolymers and biomolecules such as cellulose, soluble starch, ovalbumin, bovine serum albumin, and dopamine are also known to promote the formation and/or stabilization of vaterite by adsorbing to the surface of the crystals, changing the surface energy and retarding the dissolution and recrystallization into calcite [21,22,48].

2.3. Approaches for loading molecules into $CaCO_3$ crystals

The three main approaches for loading the molecules of interest (MOI) into the $CaCO_3$ crystals are: adsorption, infiltration and co-precipitation [50,85,86]. More recently, freezing-induced loading, which can be considered a sub-type of infiltration, has been proposed as an efficient loading route [27].

2.3.1. Adsorption

This method corresponds to the adsorption of the molecule of interest on the surface of the crystals driven by molecular interactions (Fig. 7) [50]. This type of loading is universal for all $CaCO_3$ preparation approaches and is usually done by mixing $CaCO_3$ crystals with a solution containing the MOI [85]. pH is an important parameter when adsorbing proteins into $CaCO_3$ as it affects the net charge of proteins and $CaCO_3$, and consequently the electrostatic interactions as well as the activity of the proteins [34,47]. Interestingly, despite electrostatics governing the protein-$CaCO_3$ interaction, the crucial interactions for protein loading into the vaterite crystals are the inter-protein interactions in solution [87]. This is because protein aggregates, typically presented in protein solutions, can significantly affect protein diffusion into the porous vaterite crystals and this will determine protein loading as a whole [87].

The adsorption approach is easily done, although a very long mixing time might affect the stability of the $CaCO_3$, mainly if a metastable polymorph is used. Moreover, adsorption presents a limited loading capacity [85].

2.3.2. Infiltration

The infiltration is based on mixing $CaCO_3$ crystals with the MOI followed by decreasing the MOI solubility by changing the pH or *via* solvent evaporation (Fig. 8) [50,88]. As well as adsorption, infiltration can be carried out utilising $CaCO_3$ crystals prepared by any of the different synthesis methods. However, this loading approach allows to load much higher quantities of the MOI than the adsorption approach, because the empty pores of the crystals can be completely occupied by the MOI [50,89,90].

Freezing-induced loading can be considered a sub-type of infiltration. This method involves mixing $CaCO_3$ crystals with the solution containing the MOI, which is then submitted to freezing/thawing cycles under agitation [27]. By controlling the number of cycles, the authors were able to load three to four times more nanoparticles and proteins, respectively, in comparison with the co-precipitation and adsorption methods.

2.3.3. Co-precipitation

The co-precipitation is based on capturing the MOI into the crystals during $CaCO_3$ synthesis by adding the MOI to the solutions of the precursor salts used (Fig. 9) [50,85]. This approach is widely used for the encapsulation into the crystals prepared by the solution precipitation and reverse emulsion methods. This is the most popular method for loading as it is quick, simple and allows to load very high amounts of MOI with a uniform distribution and at mild synthesis conditions [35,50,85]. Nonetheless, the cargo added during the synthesis might affect the crystallization process (nucleation rate, crystal polymorph type, crystal size and shape) and stability of $CaCO_3$. Furthermore, while on one hand this approach can result in an enormous amount of MOIs loaded (more than 60% w/w for catalase), on the other hand the synthesis conditions (precursor salts and pH) can affect the activity of some MOIs like enzymes and proteins [34,36,89,91]. The loading of small molecules might also be problematic as they can easily diffuse through the pores of vaterite (mesoporous structure with typical pore

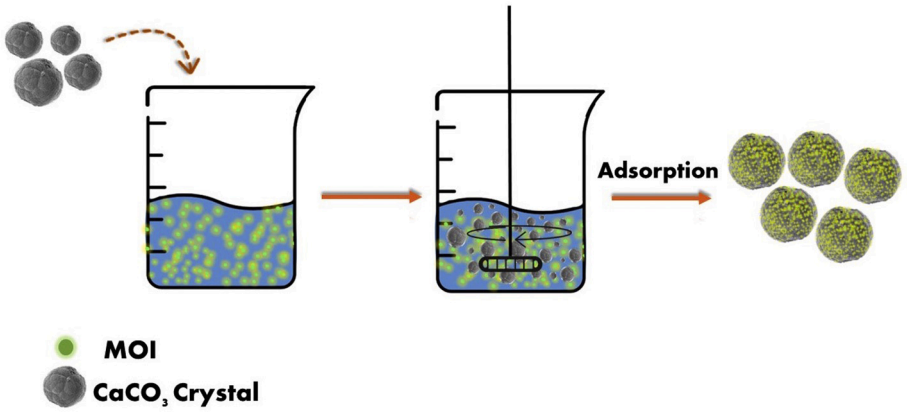

Fig. 7. Schematic representation of $CaCO_3$ crystals loading by adsorption. MOI - molecule of interest.

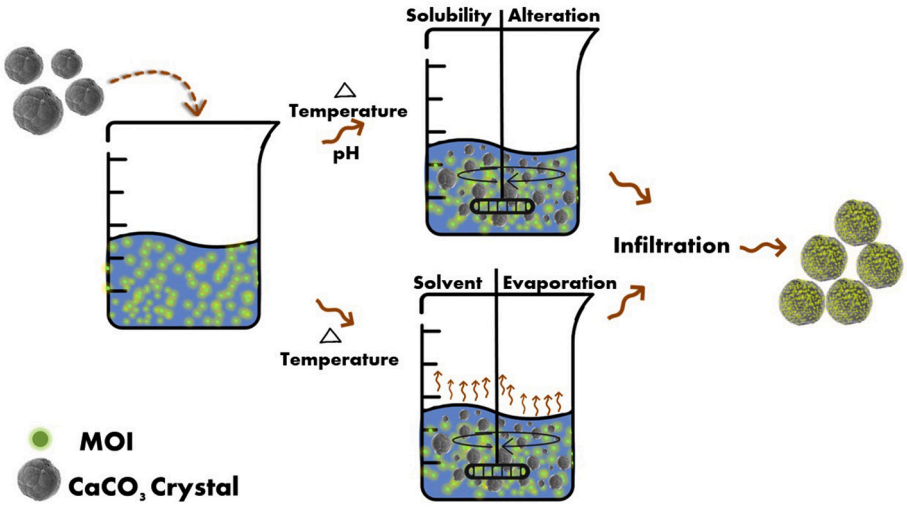

Fig. 8. Schematic representation of $CaCO_3$ crystals loading by infiltration. MOI - molecule of interest.

sizes of tens of nm). However, this can be suppressed by associating them with macromolecules [50]. An example includes loading mucin into vaterite crystals that brings extra charge into the cavity of the porous crystals making them effective for loading small drugs like doxorubicin [92–94].

2.4. Hybrid $CaCO_3$ crystals

The addition of additives during the synthesis of $CaCO_3$ can be applied to control the nucleation process and crystal stability, but also to improve the MOI loading efficiency and release profile. Coating $CaCO_3$ crystals with different polymers after synthesis can also be used to load, retain and control MOI release in a stimuli-responsive manner. Polyelectrolyte multilayers prepared by the layer-by-layer (LbL) deposition have been reported as an effective way to synthesize hybrid and polymer $CaCO_3$-based carriers for drug delivery.

Polyelectrolyte multilayers are very attractive coatings that can endow multiple functions including cellular adhesion and other bio-related activities serving as reservoirs for MOI [95–97]. The multilayers can reach thicknesses of micrometres and more [98], and host a very high amount of MOI including small charged molecules [99], large biomacromolecules such as proteins [100], and polysaccharides with rather small charge [101]. The multilayers performance can easy be tuned by changing the number of deposited layers, the type of polyelectrolytes used, including their combination, and the deposition conditions such as temperature [102]. Potentially any decomposable particle (core), including protein aggregates, can be used for the production of multilayer structures [103–105]. $CaCO_3$ crystals have been used as sacrificial cores for the formation of free-standing multiplayer capsules, as they can be easily decomposed with acidic compounds or Ca^{2+} chelating agents. The capsules can be stained by fluorescent probes bound to polyelectrolytes and the multilayers can be effective for protecting a loaded MOI and adjusting its release kinetics [106]. In general, the hybrid structures made of $CaCO_3$ crystals, polyelectrolyte multilayers, and soft polymer-bases structures sensitive to external triggers [107], can serve as mimics of biological structures such as the extracellular matrix and the intracellular environment [108], or even be a key part of tailor-made polymer-based scaffolds used for tissue engineering [109–112]. This topic is, however, out of the main scope of the review and is only briefly mentioned to demonstrate the potential use of $CaCO_3$ crystals for design of polymer and hybrid structures as advanced drug delivery carriers.

3. $CaCO_3$ crystals as vectors for antimicrobials delivery

$CaCO_3$ presents a set of characteristics that makes it an excellent candidate for drug delivery including delivery of antimicrobials, as some of these therapeutic agents present limited stability, solubility, bioavailability, distribution/penetration, and short half-life. Different research works have explored the use of $CaCO_3$ as a vector for

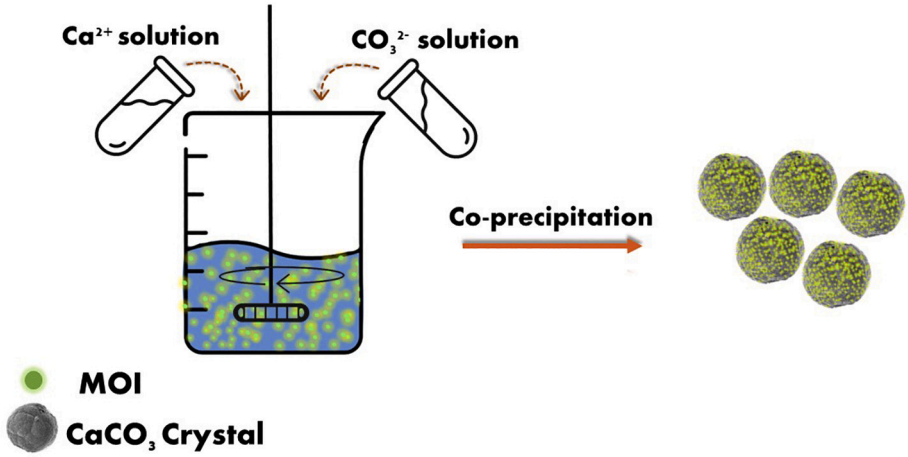

Fig. 9. Schematic representation of $CaCO_3$ crystals loading by co-precipitation. MOI - molecule of interest.

Table 1
Summary of $CaCO_3$ synthesis conditions by carbonation and characteristics of the $CaCO_3$ crystals loaded with the antimicrobial agents.

Ref.	Synthesis conditions						Antimicrobials		Crystals characteristics		
	Synthesis method	Reagents (C_i before mix.)	Temp. (°C)	pH	Reaction time	Additives	Antimicrobial agent	Loading method	Morphology	Polymorph	Size
Pan et al. [113]	Carbonation	$Ca(OH_2)$ (n.d.) CO_2- 40 ml.min^{-1}	RT[b]	–	–	EDTA (n.d.)	Gentamicin sulfate (31.17 ± 1.66 to 50.05 ± 1.85 wt%[a])	Adsorption	Chain-like	Calcite	62.5 nm
Sahoo P. et al. [114]	Carbonation	$CaCl_2$ (0.3 M) NH_4OH (5 M) CO_2 (99%)-1.5 l.min^{-1}	RT[b]	–	30 min	Microalgae cells (1.8 wt %)	AgNPs (20-25 nm; 3.7 wt%[a])	AgNPs *in situ* synthesis	Spherical	Calcite, vaterite	5 μm

RT: Room Temperature;C_i: initial concentration; mix: mixture; Temp.: Temperature; n.d.: not defined.AgNPs: Silver Nanoparticles.
[a] Weight percentage of the antimicrobial agent in the total weight of the loaded $CaCO_3$ particles.
[b] Calculated/Assumed based on the data/information presented in the article.

antimicrobials delivery. Tables 1–4 present a summary of the published research works in the area including the synthesis conditions, loading methods, and properties of the final $CaCO_3$ carriers. In the next sections, the application of the $CaCO_3$ crystals for antimicrobials delivery will be discussed in more detail.

3.1. Production of $CaCO_3$ vectors

As previously referred, there are a few different approaches for the synthesis of $CaCO_3$ crystals. In the works reporting the application of $CaCO_3$ crystals as carriers for antimicrobials the solution precipitation synthesis method was the most used. The microemulsion and carbonation methods were also reported, although not to such a great extent. Some works also presented a top-down approach for the production of micro- and nano-particles of $CaCO_3$ where cockle shells and eggshells were used as stocks [130,132,133]. Isa et al. [130] produced aragonite nanoparticles from cockle shells through a microemulsion (O/W) system using a high-pressure homogenizer for milling the particles. The particles were then loaded with ciprofloxacin by adsorption and tested against *Salmonella Typhimurium* ATCC 14028 by the disc diffusion susceptibility assay. The results demonstrated that the encapsulated ciprofloxacin presented higher antibacterial activity against *Salmonella Typhimurium* than the pristine ciprofloxacin with inhibitions zones of 18.6 ± 0.5 mm and 11.7 ± 0.9 mm, respectively. Another interesting top-down approach was reported by Apalangya et al. [132] who used eggshells waste for extraction of $CaCO_3$ and embedded proteins followed by *in situ* synthesis of silver nanoparticles (AgNPs) by ball milling. This method allowed to decrease the size of $CaCO_3$ particles and the simultaneous reduction of Ag^+ to Ag^0 by the eggshell proteins (Fig. 10) also responsible for the stabilization of AgNPs.

The different routes of $CaCO_3$ synthesis, and their easy implementation and modification, broadens the spectrum of applications of $CaCO_3$ and highlights their suitability and adaptability for the encapsulation of different types of drugs.

3.2. Loading of antimicrobials

Tables 1–4 show various methods for loading antimicrobials into the $CaCO_3$ crystals. The most used methods were adsorption and co-precipitation due to their straightforwardness, efficiency and mild loading conditions.

The efficiency of antimicrobials loading is presented in the tables and ranged between 0.015 [125] and 50 wt% [113]. This wide range is explained by the enormous number of conditions that can potentially influence the loading capacity of the crystals: crystal synthesis and loading methods, additives used, crystals size, surface area, antimicrobial agent, *etc.*

Despite the advantages of the adsorption and co-precipitation loading methods due to their easy operation, some works have reported very different and interesting loading approaches. To the best of our knowledge, Luca A. et al. [46,119,135] was the first group to report the use of $CaCO_3$ crystals as vectors for controlled delivery of antibiotics. In the different works published by the group, aragonite crystals were first synthesized and then the antimicrobials were loaded through integration by a cold isostatic pressing and sublimation process. As depicted in Fig. 11, the process starts by mixing aragonite powder with a pore-making agent (naphthalene) and the antibiotic of interest. Then the mixture is submitted to a cold isostatic pressing followed by heating under vacuum at 80 °C for the pore former elimination and the macroporosity induction [119,135].

The authors also tested the loading of the antibiotic gentamicin after aragonite processing with naphthalene. Nonetheless, the loading efficiency (Table 1) and release profiles were not satisfactory: 4 days against 8 to 12 days when gentamicin was incorporated during the aragonite processing [119].

Ferreira et al. [134] used a loading method that resembles the LbL assembly approach to produce multilayer capsules (Fig. 12). It consisted in coating the $CaCO_3$ crystals pre-coated with appositively charged polymers, PSS and polyethyleneimine (PEI), with the biocide benzyldimethyldodecylammonium chloride (BDMDAC). The antimicrobial activity of the assembled particles was tested against *Pseudomonas fluorescens* due to its ability to form disinfectant-resistant biofilms. The $CaCO_3$ crystals coated with BDMDAC promoted a reduction of viable counts between 81.9 and 93.3% for 6.33 and 11.75 mg/l of BDMDAC, respectively. Similar results were obtained with free BDMDAC: 84.9% for 6.33 mg/l, and 91.3% for 11.75 mg/l. These results demonstrated that $CaCO_3$ did not affect the antibacterial activity of BDMDAC against *P. fluorescens*.

Sahoo P. et al. [114] fabricated and loaded AgNPs into $CaCO_3$ crystals ($CaCO_3$-AgNPs), previously synthesized by carbonation and using microalgae as bio-templates (Fig. 13).

The synthesized $CaCO_3$-AgNPs particles were then mixed with paints and tested against *Escherichia coli*, *Psychrobacter alimentarius*, and *Staphylococcus equorum* using the zone of inhibition test. The results demonstrated that while the unmodified paint did not present any antimicrobial activity, the paint mixed with $CaCO_3$-AgNPs did. Padmanabhuni R. and co-workers [131] reported a singular loading approach by combining adsorption with *in situ* synthesis. The research group coated $CaCO_3$ microcrystals with 4,4-dimethylhydantoin undecanoic acid (DMH- UA) and then treated the particles with diluted bleach for the synthesis of the antimicrobial agent 3-chloro-4,4-dimethylhydantoin undecanoic acid (Cl-DMH-UA).

All the works discussed in this section demonstrate the versatility of $CaCO_3$ loading routes, and that $CaCO_3$ crystals allow the application of very different approaches.

Table 2
Summary of $CaCO_3$ synthesis conditions by reverse microemulsion, and characteristics of the $CaCO_3$ crystals loaded with the antimicrobial agents.

	Synthesis conditions						Antimicrobials		Crystals characteristics		
Ref.	Synthesis method	Reagents (C_i before mix.)	Temp. (°C)	pH	Reaction time	Additives	Antimicrobial agent	Loading method	Morphology	Polymorph	Size
Qian et al. [115]	Reverse microemulsion	$CaCl_2$ (1 M) Na_2CO_3 (1 M)	RT[b]	–	–	–	Validamycin (11.1 to 19.3 wt%[a])	Co-precipitation	Spherical	Calcite	57.5–199.7 nm
Dizaj S. et al. [9]	Reverse microemulsion	$CaCl_2$ (5 M) Na_2CO_3 (2 M)	RT[b]	–	24 h	–	Ciprofloxacin HCl (20.49 ± 0.09 wt%[a])	Co-precipitation or adsorption (10 min)	Spherical	Calcite, vaterite	90 nm (adsorption) 116 nm (co-precipitation)
Dizaj S. et al. [11]	Reverse microemulsion	$CaCl_2$ (5 M) Na_2CO_3 (2 M)	25	–	24 h	–	Gentamicin Sulfate (25.3 ± 2.5 wt%[c])	Co-precipitation or adsorption (10 min)	Spherical	Calcite, vaterite	90 nm (adsorption) 113 nm (co-precipitation)
Memar Y. et al. [116]	Reverse microemulsion	$CaCl_2$ (5 M) Na_2CO_3 (2 M)	25	–	24 h	–	Gentamicin Sulfate (25.3 ± 2.5 wt%[c])	Co-precipitation	Spherical	Calcite, vaterite	113 nm

RT: Room Temperature; C_i: initial concentration; mix: mixture; Temp.: Temperature; n.d.: not defined.
[a] Weight percentage of the antimicrobial agent in the total weight of the loaded $CaCO_3$ particles.
[b] Calculated/Assumed based on the data/information presented in the article.

3.3. Properties of $CaCO_3$ vectors

$CaCO_3$ crystals can be presented as three different anhydrous polymorphs (calcite, vaterite and aragonite) and their size can be tuned by varying the synthesis conditions. The works reported in Tables 1–4 show that the crystals loaded with antimicrobials present different characteristic due to $CaCO_3$ sensitivity to the synthesis conditions such as the type of additive, pH, temperature, reagents ratios and concentrations. $CaCO_3$ crystals loaded with antimicrobials presented spherical, rhombohedral, needle-like, chain-like, and scalenohedral morphologies, with spherical shape being the most frequently reported. The three types of polymorphs were used as carriers with some articles reporting both vaterite and calcite polymorphs. The synthesis and loading conditions, including duration, are critical factors influencing the type of polymorph produced. The long synthesis and loading times reported in some of the works presented in Tables 1–4 might explain, in some cases, the predominance of calcite and calcite/vaterite mixtures over pure vaterite crystals, as bare vaterite and aragonite crystals can recrystallize to calcite by the dissolution and recrystallization pathways within hours [136,137].

Tables 1–4 show that the size of $CaCO_3$ crystals loaded with antimicrobial agents ranged between ca 14 nm and 10 μm. The vector size is an important parameter that can affect the pharmacokinetics of the whole system including the carrier distribution, extravasation/diffusion, endocytosis, flow properties, and clearance [138]. Therefore, the size of the crystals should be controlled based on their application especially if developed for human or animal use. Microparticles for subcutaneous or intramuscular administration generally present diameters up to 50 μm [139], nonetheless, for intravenous administration particles should have sizes between 30 and 300 nm as particles smaller than 10 nm are rapidly excreted by the kidneys and particles larger than 300 nm can promote thrombosis and be rapidly eliminated [140]. For pulmonary drug administration, the carriers optimum size ranges between 1 and 5 μm [138]. Smaller delivery systems present cytotoxic effects and are easily exhaled without promoting any therapeutic action. On the other side, particles with diameters larger than 5 μm are removed by the mucociliary clearance mechanism, not fulfilling their action [138]. The simplicity with which it is possible to adjust the size of $CaCO_3$ crystals by just changing few synthesis parameters (*e.g.*, reagents concentration, stirring speed and time) makes the crystals attractive and dynamic drug delivery systems for different targets and routes of administration.

Islan G. and co-workers [117,118] published two works where $CaCO_3$ crystals with the optimal size for pulmonary delivery were developed. The hybrid vaterite microparticles, with sizes between 3 and 5 μm included sodium alginate (120 kDa) and/or high methoxyl pectin (70–75% esterification degree) [117,118]. A summary of the synthesis conditions and particle characteristic are present in Table 3. After synthesis the crystals were treated with alginate lyase (AL) for alginate cleavage (Fig. 14) resulting in particles with much higher surface area (71.6 to 74.9 m^2/g) than the bare $CaCO_3$ (16.4 m^2/g) and untreated crystals (34.9 to 51.4 m^2/g) [117]. The developed particles were loaded with levofloxacin or levofloxacin/deoxyribonuclease (DNase) and tested against *Pseudomonas aeruginosa* ATCC 15442. The results demonstrated that the microparticles treated with AL present a potent bacterial inhibition resultant from the particles increased surface area and consequent higher levofloxacin content. Further *in vivo* experiments were carried out in mice to study the distribution and preclinical pharmacokinetics of the particles administrated in the lungs *via* nebulization and dry powder inhalation. The particles presented a good penetration resulting in higher levels of levofloxacin in comparison with the administration of the free drug form [118].

The tuneable properties of $CaCO_3$ crystals demonstrate their versality to deliver drugs into different targets and the possibility to finely adjust their pharmacokinetic and release mechanism.

Table 3
Summary of $CaCO_3$ synthesis conditions by solution/colloidal precipitation, and characteristics of the $CaCO_3$ crystals loaded with the antimicrobial agents.

	Synthesis conditions						Antimicrobials		Crystals characteristics		
Ref.	Synthesis method	Reagents (C_i before mix.)	Temp. (°C)	pH	Reaction time	Additives	Antimicrobial agent	Loading method	Morphology	Polymorph	Size
Islan G. et al. [117]	Colloidal precipitation followed by AL treatment (48 h)	Na_2CO_3 (0.30 M) $CaCl_2$ (0.29 M)	–[b]	10	5 min (CP) 48 h (AL treatment)	Glycine buffer; sodium alginate and/or pectin (6.5–23.6 wt %)	Levofloxacin (1.21 ± 0.01 to 1.40 ± 0.06 wt%[c])	Adsorption (24 h)	Spherical	Vaterite	3.6–4.6 μm
Islan G. et al. [118]	Colloidal precipitation followed by AL treatment (48 h)	Na_2CO_3 (0.30 M) $CaCl_2$ (0.29 M)	–[b]	10	5 min (CP) 48 h (AL treatment)	Glycine buffer; sodium alginate (n.d.) and DNase (1.15–2.71 wt%)	Levofloxacin (7.41 wt%[c])	Adsorption (24 h)	Spherical	Vaterite	3–5 μm
Lucas et al. [46]	Solution precipitation	$KHCO_3$ (0.1 M) $CaCl_2$ (0.1 M)	100	–	–	–	Gentamicin sulfate (n.d.); metronidazole (n.d)	Integration by CIP and sublimation	Needle-like	Aragonite	5–10 μm (L) 1 to 2 μm (W)
Lucas A. et al. [119]	Solution precipitation	$KHCO_3$ (0.1 M) $CaCl_2.2H_2O$ (0.1 M)	100	–	–	–	Gentamicin Sulfate: integration (5.5 ± 0.2 to 11.2 ± 0.6 wt%[a]); adsorption (0.35 ± 0.02 to 0.40 ± 0.02 wt%[a])	Integration by CIP (5 min 600 MPa) and sublimation; adsorption	Needle-like	Aragonite	5–10 μm (1 to 2 μm (W)
Yan H. et al. [120]	Solution precipitation	$CaCl_2$ (2 mM) Na_2CO_3 (2 mM)	0, 20, 40	–	24 h	Guar Gum (n.d.)	Vancomycin hydrocholoride (24.3 to 46 wt%[a])	Adsorption (12 h)	Spherical	Calcite,vaterite	1 μm
Dizaj S. et al. [75]	Solution precipitation	Na_2CO_3 (n.d.): $CaCl_2$ (n.d.) molar ratios - 1:1; 3:1.5; 5:2	RT[c]		15 min	–	Gertamicin Sulfate (n.d.)	Co-Precipitation	–	–	80.0–300.12 nm
Begum et al. [26]	Solution precipitation	$(NH_4)_2CO_3$ (n.d.): $CaCl_2$ (n.d.) molar ratios - 1:1	RT	–	30 min	Poly (L-asp) and penta (L-lys) (n.d.)	Tetracycline (n.d.)	co-Precipitation	Spherical	Vaterite, amorphous	0.5–1 μm
Mihai et al. [121]	Solution precipitation	Na_2CO_3 (0.05 M) $CaCl_2.2H_2O$ (0.10 M)	RT	10.5	9 h	PAH and/or pectins (n.d.)	Tetracycline hydrocholoride (15.28–39.90 wt%[c])	Adsorption (4 h)	Rhombohedral and spherical	Calcite, vaterite	4.85–7.76 μm
Racovita et al. [122]	Solution precipitation	Na_2CO_3 (0.05 M) $CaCl_2.2H_2O$ (0.10 M)	RT	10.5	8 h	PAH and/or pectins (n.d.)	Streptomycin (3.54–15.79 wt%[c]); kanamycin (4.43–29.52 wt%[c])	Adsorption (4 h)	Rhombohedral and spherical	Calcite, vaterite	~5–8 μm
Said F. et a. l [123]	Solution precipitation	Na2CO3 (0.33 M) CaCl2 (0.33 M)	RT[c]	–	3 min	–	Penicillin; ampicillin; ciprofloxacin (> 5 wt%[a]b)	Adsorption (24 h)	Spherical	Calcite, vaterite	5 μm
Matei et al. [124]	Solution precipitation	Na_2CO_3 (0.4 M) $CaCl_2$ (0.4 M)	10	–	30 min	*Ulva lacuna* extract (n.d.)	Ag/AgCl (n.d.)	Co-precipitation	Spherical or rhombohedral	Calcite	–
Długosz M. et al. [125]	Solution precipitation	Na_2CO_3 (0.03 M) $Ca(NO_3)$ (0.03 M)	25	–	5 min	PSS and PAH (after synthesis) (n.d.)	AgNPs (30-50 nm; 0.015 wt% [a])	Co-precipitation	Spherical	–	2 μm
Baldassarre et al. [126]	Solution precipitation	$NaHCO_3$ (0.125 M) $CaCl_2$ (0.083 M)	–	–	–	–	Caffeic acid; *N*-acetylcysteine (n.d.)	Adsorption (overnight)	–	–	50–75 nm
Tessarolo L. et al. [127]	Solution precipitation	$CaCl_2$ (0.025 M) Na_2CO_3 (0.05 M)	30	–	72 h	SDS and Pluronic F-68 (n.d.)	Benznidazole (25 wt%[a])	Co-Precipitation	Spherical	–	41.81 nm
Min K. et al. [128]	Solution precipitation	$CaCl_2$ (0.044 M)[c] Na_2CO_3 (0.044 M)[c]	RT	8	16 h	PEG-PAsp (n.d.)	Doxycycline hyclate (2.35 wt% [a])	Co-precipitation	Spherical	Vaterite	312.5 nm
Xue et al. [129]	Solution precipitation	$CaCl_2$ (0.2 M) Na_2CO_3 (0.2 M)	RT[c]	–	30 min	β-cyclodextrins; casein and Fe_3O_4 nanoparticles (n.d.)	Minocycline (n.d.)	Adsorption (24 h)	Spherical	Vaterite	2–5 μm

RT: Room Temperature; C_i: initial concentration; mix: mixture; Temp.: Temperature; n.d.: not defined; AL: Alginate lyase; CP: Colloidal precipitation; CIP: Cold isostatic pressing; L-Length; W-With; DNase: deoxyribonuclease; Poly(L-asp): Poly(L-aspartic acid sodium salt); penta(L-lys): Penta(L-lysine hydrobromide); PAH: Poly(allylamine hydrochloride); AgNPs: Silver Nanoparticles; PSS: Poly(sodium 4-styrenesulfonate); PEG-PAsp: poly(ethylene glycol)-poly(aspartic acid).

[a] Weight percentage of the antimicrobial agent in the total weight of the loaded $CaCO_3$ particles.

[b] Synthesis temperature is not specified, but the use of an ice bath is reported.

[c] Calculated/Assumed based on the data/information presented in the article.

3.4. Release of antimicrobials

The antimicrobials currently used for the treatment of infectious diseases present some problems including short half-life, limited stability and solubility. Moreover, the therapeutic range of some drugs is narrow, as high concentrations can be toxic whereas low concentrations can promote the development of antimicrobial resistance [141,142]. Drug delivery systems can improve the pharmacokinetics of antimicrobial drugs by protecting and offering the control over their release in order to decrease dosage frequency, side effects and improve the therapeutic effect.

Drug delivery systems release the cargo through diffusion and/or carrier alterations in response to an intrinsic stimuli characteristics of pathological areas (pH, temperature, redox conditions and expression of certain enzymes) or an external stimuli applied deliberately (magnetic field, heat, light and ultrasound) [143]. $CaCO_3$ carriers can release the cargo *via* three ways: diffusion, carrier dissolution and recrystallization of the metastable polymorphs (vaterite and aragonite) to the more stable form, *i.e.*, calcite. The drug release usually occurs by the three pathways, although the carrier and cargo properties and interactions, allied with the medium conditions as pH, chemical composition and temperature, will affect the primary release mechanism.

pH is a critical parameter on the $CaCO_3$ solubility. At low pH values free protons react with CO_3^{2-} forming HCO_3^- and consequently dissolving $CaCO_3$ crystals and therefore promoting the release of the drug. pH has been used as a trigger for $CaCO_3$ cargo release in acidic tumour microenvironments and inflammation sites [86,128,144].

Bacterial infection sites usually present low pH values due to increased amount of organic acids resultant from the anaerobic fermentation in certain bacteria and the host immune system response [145–147]. Together, the bacterial metabolism and the immune response can decrease the pH up to 5.5 [146]. Some of the works reporting the use of $CaCO_3$ crystals as antimicrobial carriers explore the pH sensitivity to trigger the drug release.

Min K. and co-workers [128] synthesized $CaCO_3$ nanoparticles loaded with doxycycline hyclate (DOXY) by co-precipitation using PEG-PA co-polymer as a mineralization template (Fig. 15). The goal was to synthesize pH-sensitive nanoparticles selective to the acidic microenvironment of bacterial biofilms. The drug release was tested at pH 7.4, 6.5, 5.5 and 4.0 resulting in ca 20, 60, 90 and 100%, respectively, of the drug being released after 24 h (Fig. 17). The results demonstrated the pH-dependent release behaviour of the carrier, with acidic pH triggering the release of DOXY due to an increased solubility of $CaCO_3$ at lower pH. The nanoparticles were tested against *Prevotella intermedia* ATCC49046, an anaerobic gram-negative bacterium known to cause oral diseases. The experiments were done at uncontrolled (~7.4–5.3) and controlled pH (~7.4–6.5) and with free and encapsulated DOXY. The results showed that the loaded ($CaCO_3$_DOXY) and free DOXY, at uncontrolled pH and after 25 h, had similar antibacterial activity, both presenting the same bactericidal concentration (1 μg/ml). On the other hand, at controlled pH, the drug loaded into $CaCO_3$ presented higher bactericidal concentration (2 μg/ml), demonstrating the nanoparticles sensitivity to pH. The crystal violet staining assay was also performed to investigate the inhibitory effect of DOXY-$CaCO_3$ on *Prevotella intermedia* biofilm formation. Once again, the pH-sensitivity was demonstrated with half of the antibiotic concentration significantly decreasing the biofilm formation at lower pH.

Qian et al. [115], synthetized calcite crystals loaded with validamycin by the reverse microemulsion method. The main synthesis conditions and crystals properties are present in Table 2. The release behaviour and stability of the free and encapsulated validamycin forms were tested at three different pH values: 5; 7 and 9. The results showed that validamycin loaded into $CaCO_3$ crystals presents better stability and a controlled release profile. At pH 5,7 and 9 almost all validamycin was released after 7 and 14 days demonstrating a pH-dependant release behaviour.

Table 4
Summary of the fabrication conditions for top-down method or previously acquired $CaCO_3$ crystals, and characteristics of the $CaCO_3$ crystals loaded with the antimicrobial agents.

Ref.	Fabrication conditions				Antimicrobials		Crystals characteristics		
	Method	Material	Temp. (°C)	Additives	Antimicrobial agent	Loading method	Morphology	Polymorph	Size
Isa et al. [130]	Top-down, microemulsion (O/W) milling with HPH	Dried cockle shells-$CaCO_3$ powder	RT[b]	–	Ciprofloxacin HCl (5.9 wt%[a])	Adsorption (overnight)	Spherical	Aragonite	13.94–23.95 nm
Padmanabhuni R. et al. [131]	CA	$CaCO_3$	–	–	Cl-DMH-UA (n.d.)	Adsoprtion of the Cl-DMH-UA precursor (2 h), Cl-DMH-UA *in situ* synthesis (1 h) (n.d.)	Scalenoheral	Calcite[b]	2–4 μm
Apalangya et al. [132]	Top-down	Eggshells	100	–	AgNPs (5-20 nm) (n.d.)	Adsorption and *in situ* AgNPs synthesis (2 h)	–	Calcite	Micron range
Tiimob B. et al. [133]	Top-down	Eggshells	–	–	AgNPs (10-15 nm) (n.d.)	Adsorption and *in situ* AgNPs synthesis (≥ 5 h)	–	Calcite	–
Ferreira et al. [134]	CA	$CaCO_3$	–	PSS and PEI (n.d.)	Benzyldimethyldodecylammonium chloride (n.d.)	LbL adsorption	Spherical	–	2–4 μm

CA: $CaCO_3$ acquired from and external supplier; RT: Room Temperature; Temp.: Temperature; n.d.: not defined; AgNPs: Silver Nanoparticles; PSS: Poly(sodium 4-styrenesulfonate); Cl-DMH-UA: 3-chloro-4,4-dimethylhydantoin undecanoic acid; LbL: Layer by Layer; PEI: Polyethyleneimine.

[a] Weight percentage of the antimicrobial agent in the total weight of the loaded $CaCO_3$ particles.

[b] Calculated/Assumed based on the data/information presented in the article.

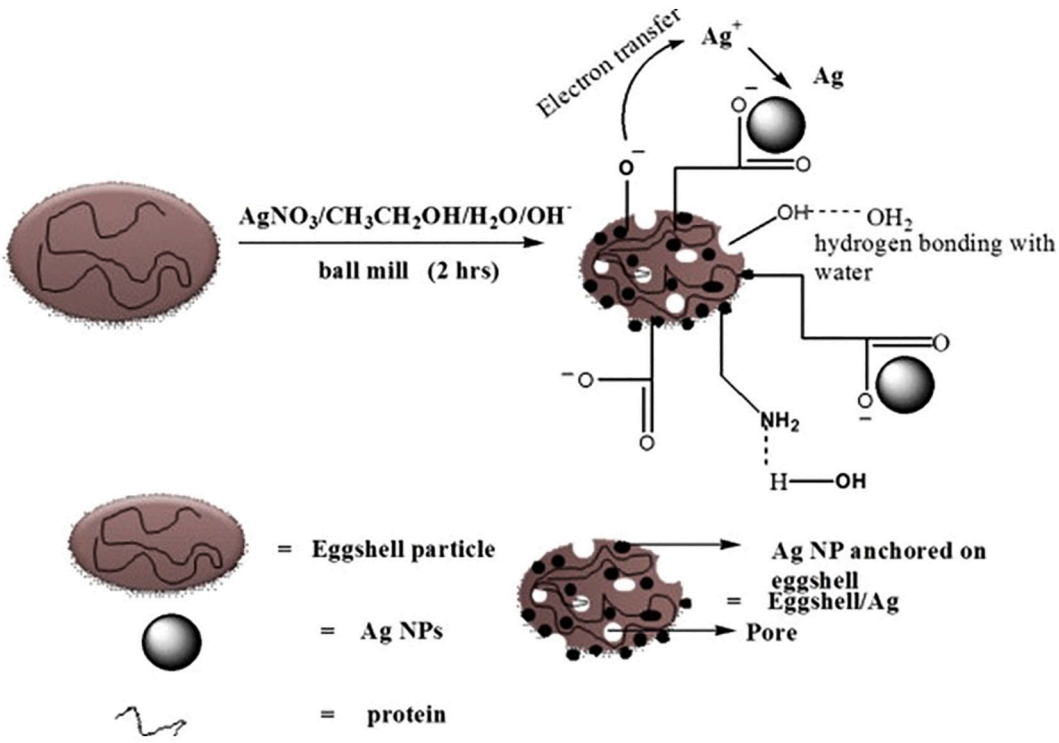

Fig. 10. Proposed mechanism of CaCO3-AgNPs nanocomposites formation. Reprinted from Apalangya et al. [132]. Copyright 2014, with permission from Elsevier.

Długosz M. and co-workers [125] fabricated $CaCO_3$ vectors loaded with AgNPs by co-precipitation and then used the particles for coating down feathers. The AgNPs release profile from $CaCO_3$ particles was evaluated at two different pH values, *i.e.*, 6.8 and 5.4 over 14 days (Fig. 17). The results demonstrated a slow and pH-dependant release of silver and, as expected, at pH 5.4 silver was released more quickly.

Begum G. and co-workers [26] developed $CaCO_3$ structures using poly(L-aspartic acid sodium salt) (poly(L-asp)), and penta(L-lysine hydrobromide) (penta(L-lys)) as templates for spherical particles formation, and tetracycline entrapment (Fig. 15).

Tetracycline release behaviour was evaluated over 15 days at three different pH values (4.5, 6.0, and 7.4) and at 37 °C (Fig. 16). Regardless of the pH, an initial burst release of the drug was verified followed by a controlled release of almost all the loaded antibiotic within 24 h at pH 4.5 (100% released) and 360 h at pH 6 (94% released). The drug release at pH 7.4 was comparatively slower with 61% of the drug being released after 360 h. This and the other research works presented in this section demonstrate the pH-sensitivity of $CaCO_3$ carriers, with low pH values being able to trigger $CaCO_3$ dissolution and consequent drug release.

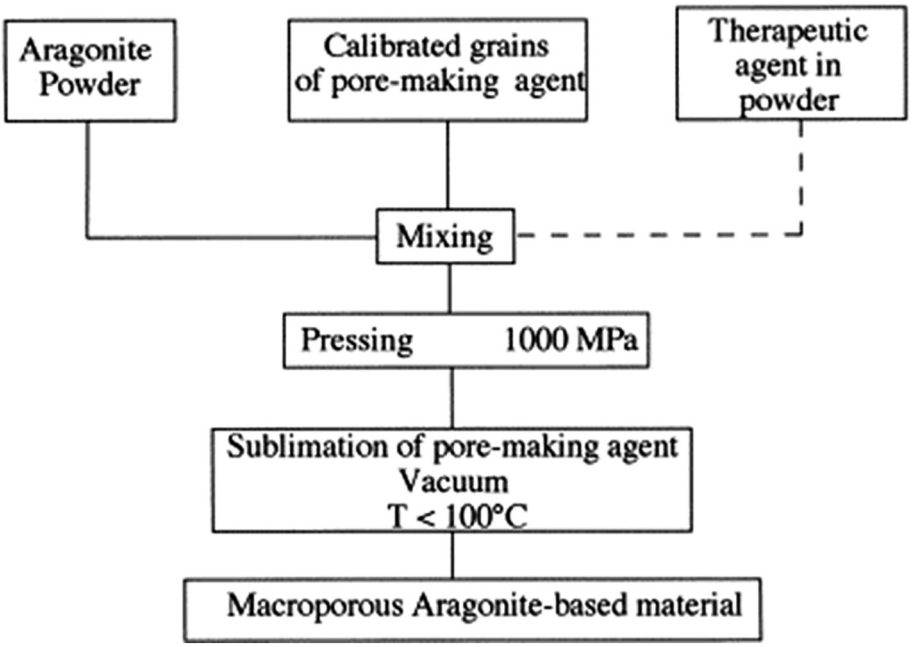

Fig. 11. Steps for the fabrication of porous aragonite-based materials. Reprinted from Luca A. et al. [46]. Copyright 2001, with permission from Elsevier.

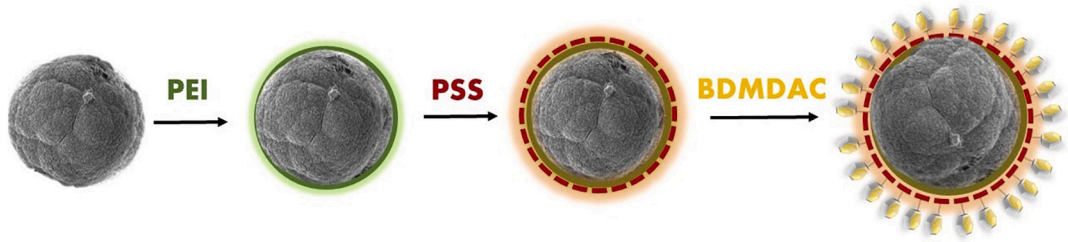

Fig. 12. Representation of the layer-by-layer assembly method used to produce $CaCO_3$ microparticles coated with BDMDAC. Figure redrawn based on the work of Ferreira et al. [134].

3.5. Biocompatibility of $CaCO_3$ vectors

The application of drug delivery systems depends on the safety that they present to the patients. Therefore, their biocompatibility assessment is of utmost importance.

Up to now, all *in vitro* studies suggest no cytotoxicity of bare vaterite crystals [148] even when used at high concentrations [149]. Although there is still a limited number of *in vivo* studies on $CaCO_3$ use, all of them suggest safe administration of $CaCO_3$ particles as drug carriers *via* different routes, *e.g.* ocular [36], intranasal [150], pulmonary [151] or transdermal [152]. Interestingly, it has been demonstrated that bolus intravenous injections of bare $CaCO_3$ crystals can alter the extracellular pH and can be used to inhibit tumour growth *in vivo* [153]. Besides, different works have tested the biocompatibility of $CaCO_3$ carriers loaded with antimicrobials. Memar M. et al. [116] synthetized $CaCO_3$ nanoparticles loaded with gentamicin sulfate by a reverse microemulsion method and tested their biocompatibility and cytotoxicity. Biocompatibility was accessed using three assays: i) haemolysis assays on human red blood cells, ii) erythrocyte sedimentation rate essay and iii) protein interaction between loaded $CaCO_3$ and human blood plasma. The toxicity was tested by the 3-(4,5-Dimethylthiazol-2-yl)-2,5-diphenyltetrazolium bromide (MTT) viability assay on a hBM-MSC cell line. The reported results demonstrated that the $CaCO_3$ nanoparticles loaded with gentamicin sulfate displayed a favourable biocompatibility and low toxicity.

Isa et al. [130] tested the biocompability and cytotoxicity of aragonite particles loaded with ciprofloxacin in a Macrophages J774A.1 cell line using three different tests: i) MTT (viability test), ii) bromo-21-deoxyuridine assay (genotoxicity test) and iii) interleukin 1 beta cellular expression assessment by RNA extraction and reverse transcriptase-polymerase chain reaction, (immunogenicity assessment). The results demonstrated that the loaded nanoparticles presented cytocompatibility without the upregulation of the immune system response.

The *in vivo* biocompatibility, resorption and bone ingrowth of aragonite microparticles was evaluated by Lucas et al. [46]. The results demonstrated an excellent biocompatibility, resorption and osteoconduction with the porosity degree largely affecting the last two properties. Overall, the results demonstrated the enormous potential of this type of material as a resorbable bone substitute and its good biocompatibility.

3.6. Antimicrobial performance

The key goals when using antimicrobials delivery systems are to protect the antimicrobials from degradation, decrease the toxicity and promote a controlled release while assuring a therapeutic concentration at the site of infection. Table 5 presents a comparison between the antimicrobial activity of the free and immobilized antimicrobial agents. In most of the reported studies the compounds loaded into $CaCO_3$ crystals presented similar or better antimicrobial activity than the free form. Several factors can alter the antimicrobial activity of the compounds loaded into $CaCO_3$ particles such as the size and morphology of the crystals, presence of additives, affinity between the $CaCO_3$ and the cargo, type of microorganism, microenvironment conditions (pH, temperature, composition and ionic strength) and even the type of antimicrobial assay used.

Apalangya et al. [132] produced $CaCO_3$ particles with embedded AgNPs and tested the free and loaded AgNPs against *Escherichia coli* ATCC 11775 by a modified Kirby-Bauer disc diffusion assay. The results indicated a superior antibacterial activity of the AgNPs loaded into $CaCO_3$ particles. The authors explained this effect by a better dispersion and interaction of the particles with *E. coli* improved by the hydrophilic groups of the eggshell proteins present in the vectors. Isa et al. [130] also reported better antimicrobial activity against *Salmonella Typhimurium* ATCC 14028, of ciprofloxacin loaded into aragonite. The authors proposed that the higher antibacterial activity resulted from a higher diffusion of the nanoparticles through the bacteria. Tessarolo L. et al. [127] published one of the few works where an antiparasitic drug, benznidazole (BZN), is encapsulated into $CaCO_3$ crystals (BZN-$CaCO_3$). The encapsulated and free drug was tested against *Trypanosoma cruzi* strain Y, a parasite responsible for the Chagas disease. The results demonstrated a higher potency of BZN-$CaCO_3$ particles against the three forms of *Trypanosoma cruzi* (epimastigote, trypomastigote and amastigote). The authors proposed that the better activity of BZN-$CaCO_3$ particles resulted from an increased cell permeability when compared with the free BZN form. Pan et al. [113] produced calcite nanoparticles

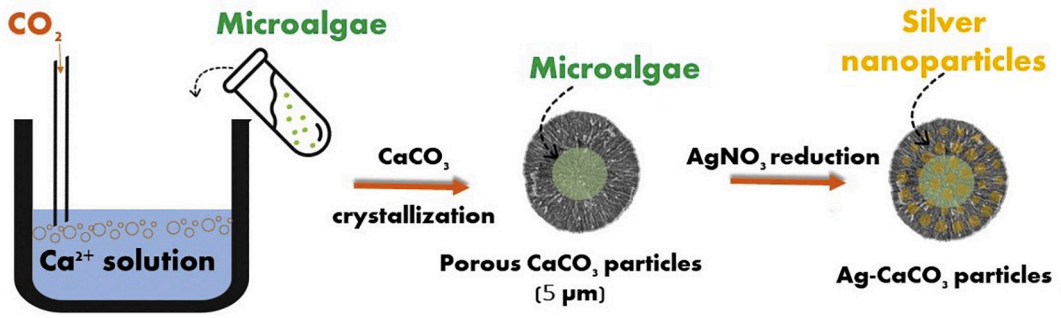

Fig. 13. Synthesis steps of porous $CaCO_3$ microsphere by carbonation in the presence of microalgae. Silver nanoparticles were synthesized on the porous microparticles by reducing $[Ag(NH_3)]^+$ with D-maltose. Figure redrawn based on the work of Sahoo P. et al. [114].

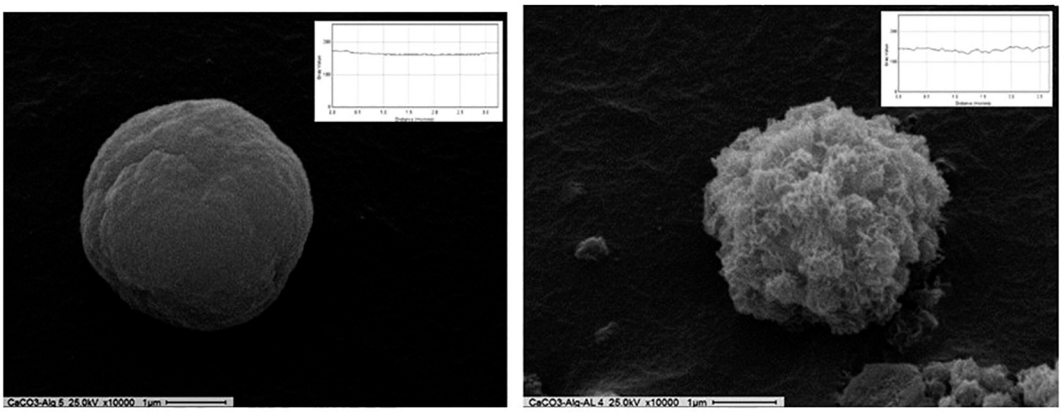

Fig. 14. SEM images of $CaCO_3$-sodium alginate microparticles before (left) and after (right) being treated with alginate lyase. Figure adapted from Islan C. et al. [117]. The plot profile of the microparticles surface is shown in the top right corner of the images. Copyright 2015, with permission from Elsevier.

loaded with gentamicin sulfate and tested the antibacterial activity of bare calcite, free and encapsulated gentamicin against *Bacillus subtillis*. The results demonstrated a synergistic effect between $CaCO_3$ and the gentamicin sulfate. The authors propose that the drug delivery system increased the damage of the bacterial cells wall and enhanced the permeability of the cell membranes. The synergistic effect was not reported by Dizaj S. et al. [9] and Memar et al. [116] who also studied the encapsulation of gentamicin in $CaCO_3$ particles and verified that the bare antibiotic presented similar and better antibacterial properties, respectively. The different results can be explained by the different properties of the carriers (size, morphology, porosity), experimental conditions and bacterium type.

Min K. et al. [128] and Padmanabhuni R. et al. [131] also reported inferior antibacterial activity of the antimicrobial agents loaded into $CaCO_3$ particles at some of the experimental conditions studied. In the case of Min K. et al. [128] the lower bactericidal activity of the

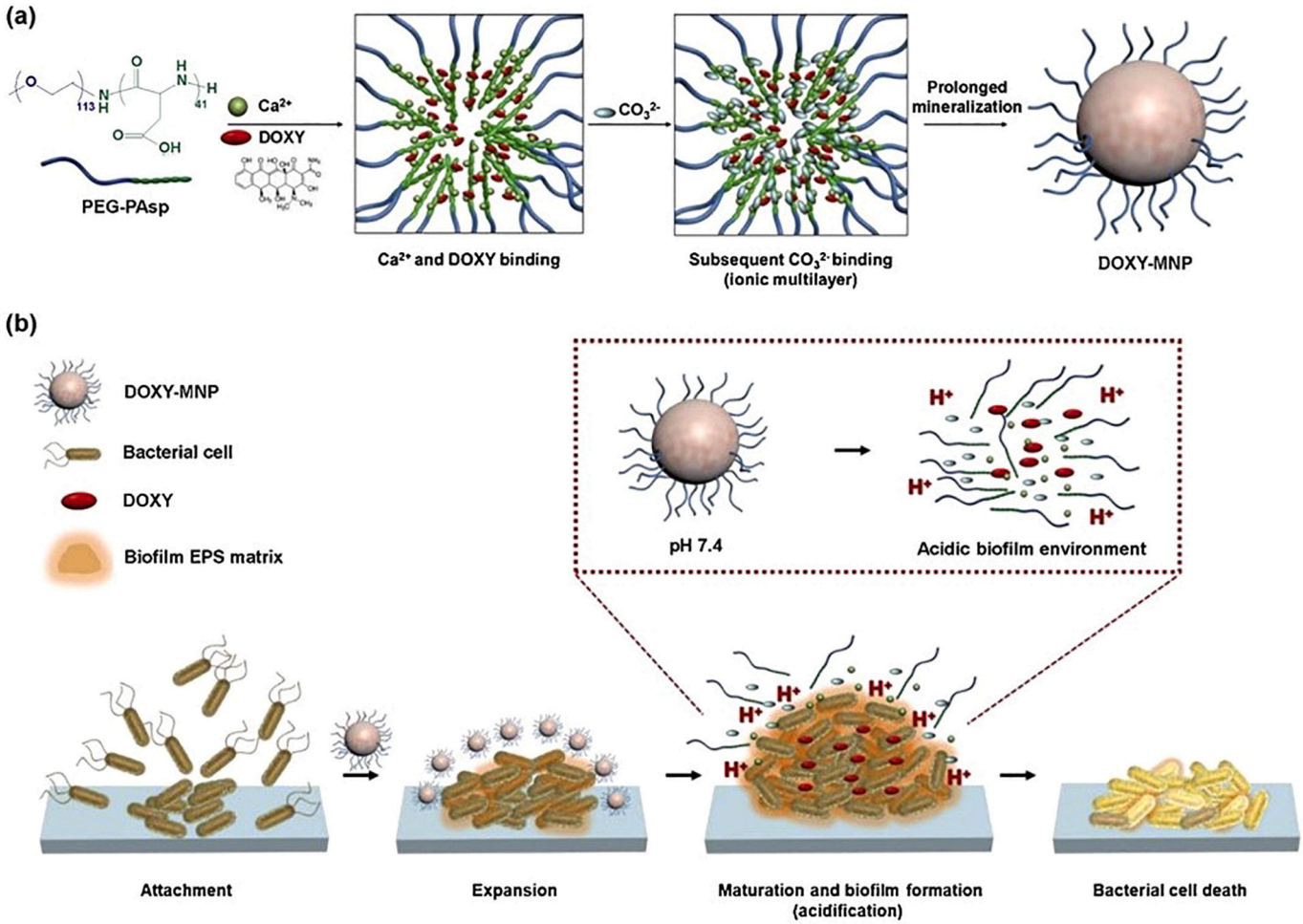

Fig. 15. Illustration of DOXY-loaded $CaCO_3$ (DOXY-MNPs) synthesis pathway (a) and DOXY release mechanism from the MNPs triggered by the acidic microenvironment of the biofilm (b). EPS: exopolysaccharides. Reprinted from Min K. et al. [128]. Copyright 2019, with permission from Elsevier.

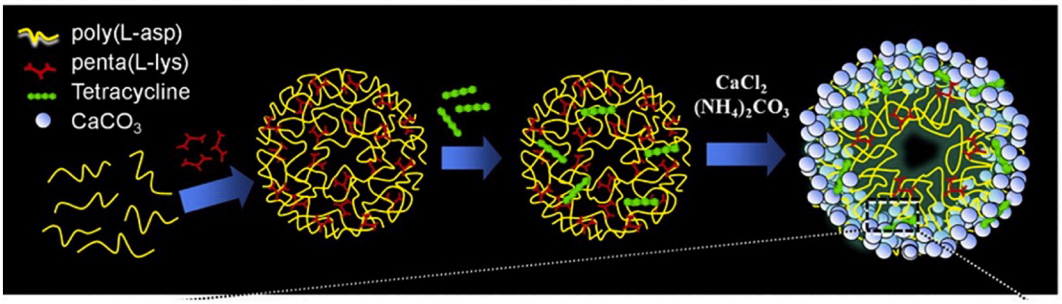

Fig. 16. Tetracycline entrapment process and $CaCO_3$ mineralization and assembly. Adapted from Begum et al. [26]. Copyright 2016, with permission from American Chemical Society.

encapsulated doxycycline hyclate was verified at a higher pH values (7.4–6.5) but not at lower ones (7.4–5.3) as discussed in Section 3.4. Regarding the work of Padmanabhuni R. et al. [131], the inferior antibacterial activity was related with the lower mobility of the antimicrobial agent on the $CaCO_3$ particles, with free Cl-DMH-UA presenting better results due to its higher mobility. Nonetheless, when free and encapsulated Cl-DMH-UA were incorporated into cellulose acetate films as antimicrobial fillers, both presented similar activity against *S. aureus* regardless of the concentration, and against *E. coli* at 5% w/w. Moreover, both systems presented a similar biofilm growth inhibition.

Overall, $CaCO_3$ has a high potential as a vector for delivery of antimicrobial agents as it can protect and promote a controlled release without affecting the antimicrobial activity.

4. Current challenges and future opportunities

$CaCO_3$ crystals present a set of characteristics desirable for drug carriers including biocompatibility, controlled release, low-cost and simple fabrication. Several works have studied the application of $CaCO_3$ crystals loaded with antimicrobial agents for different applications. Some of these research studies propose the use of the vectors for antimicrobial coatings, fillers for polymeric composite materials [125,131,133], water filtration [132], osteomyelitis treatment and bone grafting [9,11,46,116,119], treatment of respiratory infections [117,118], antimicrobial filler for paints [114], oral infections treatment [128], biocides delivery into olive trees [126], and treatment of skin burns [124]. The diverse applications reported up to now demonstrate the versatility of $CaCO_3$ crystals.

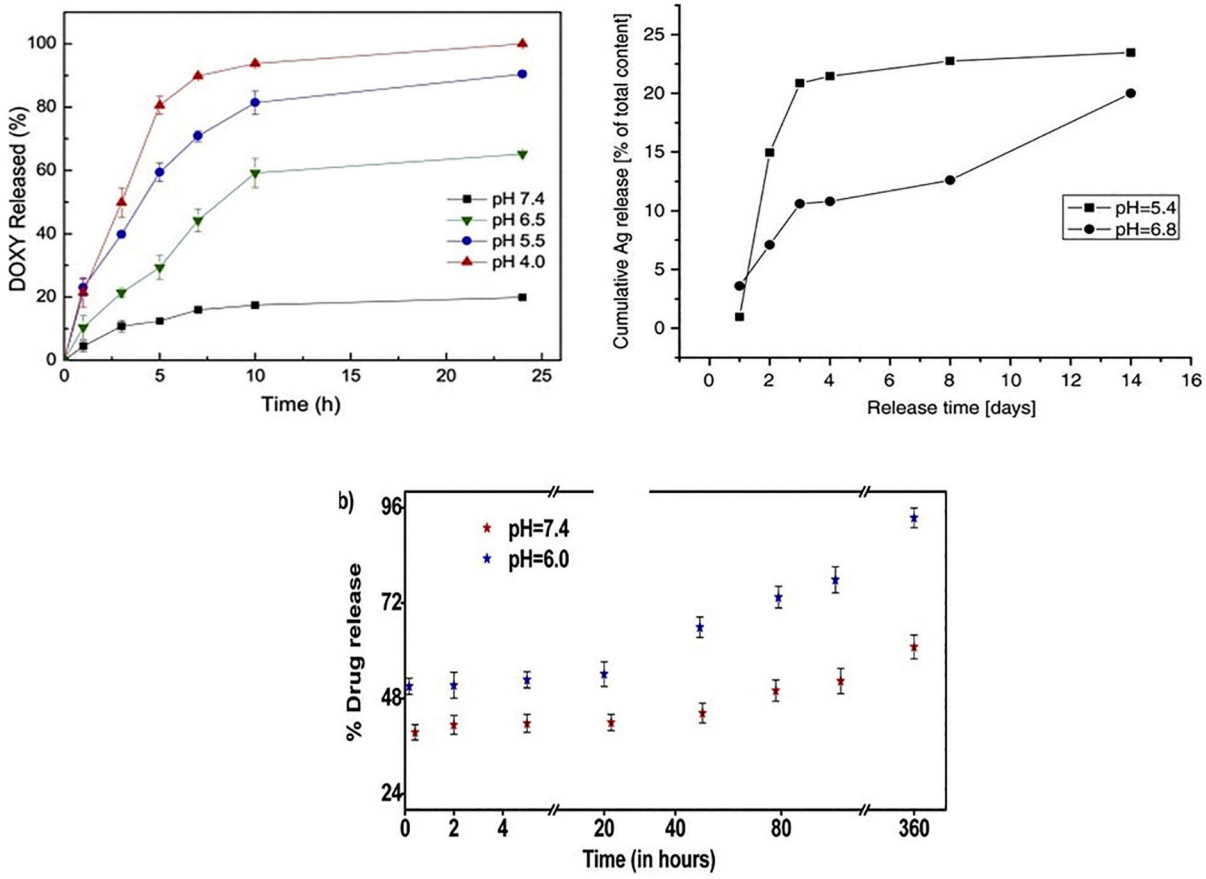

Fig. 17. pH-responsive release of doxycycline (top left), AgNPs (top right) and tetracycline (bottom) from $CaCO_3$ carriers. Adapted from Min K. et al. [128], Długosz M. et al. [125], and Begum et al. [26], respectively. Copyright 2019, 2012 and 2016, with permission from Elsevier, Springer Nature and American Chemical Society, respectively.

Table 5
Summary of the antimicrobial activity of the free and $CaCO_3$-encapsulated antimicrobial agents.

Ref.	Microorganism	Antimicrobial agent (AA)	Antimicrobial activity (Free-AA)	Antimicrobial activity ($CaCO_3$-AA)	Result type
Pan et al. [113]	*B. subtillis*	Gentamicin sulfate	−	+	GI
Qian et al. [115]	*Rhizoctonia solani*	Validamycin	+(2nd day) −(7th day)	−(2nd day) +(7th day)	GI
Dizaj S. et al. [9]	*S. aureus*	Ciprofloxacin HCl	SA	SA	MIC
Dizaj S. et al. [11]	*S. aureus*	Gentamicin sulfate	SA	SA	MIC
Memar Y. et al. [116]	*P. aeruginosa*	Gentamicin sulfate	+ SA	− SA	MIC MBC
Begum et al. [26]	*B. subtilis*, *S. aureus*, *S. epidermidis*, *E. coli*, *K. pneumoniae*, and *P. aeruginosa*	Tetracycline	SA	SA	MIC and ZI
Tessarolo L. et al. [127]	*Trypanosoma cruzi* strain Y	Benznidazole	−(24 h) SA (72 h) −	+ (24 h) SA (72 h) +	IC_{50} LC_{50}
Min K. et al. [128]	*Prevotella intermedia*	Doxycycline hyclate	SA +	SA −	BC (pH 7.4–5.32) BC (pH 7.4–6.5)
Isa et al. [130]	*Salmonella Typhimurium*	Ciprofloxacin HCl	−	+	ZI
Padmanabhuni R. et al. [131]	*S. aureus* and *E. coli*	Cl-DMH-UA	+ SA (*S. aureus*) +(*E. coli*:1–3 wt%[a]) SA (*E. coli*: 5 wt%[a]) SA	− SA (*S. aureus*) −(*E. coli*: 1–3 wt%[a]) SA (*E. coli*: 5 wt%[a]) SA	SR SR (CA) BGI
Apalangya et al. [132]	*E. coli*	AgNPs (5 − 20 nm)	−	+	ZI
Ferreira et al. [134]	*Pseudomonas fluorescens*	Benzyldimethyldodecylammonium chloride	SA	SA	SR

AA: Antimicrobial Action; SA: Similar Antimicrobial Activity; (−): Inferior Antimicrobial Activity; (+) Superior Antimicrobial Activity; GI: Growth Inhibition; MIC: Minimum Inhibitory Concentration; MBC: Minimum Biofilm Inhibitory Concentration; ZI: Zone of Inhibition; IC_{50}: Inhibitory Concentration that inhibits 50% of growth; LC_{50}: Lethal Concentration that causes the death of 50% of the microorganisms; BC: Bactericidal Concentration; SR: Survival Ratio; CA: Cellulose Acetate (free and encapsulated forms used as cellulose acetate additive); Cl-DMH-UA: 3-chloro-4,4-dimethylhydantoin undecanoic acid; BGI: Biofilm Growth Inhibition.
[a] Cl-DMH-UA weight percentage on the total weight of the cellulose acetate film.

While $CaCO_3$ can work as a vector that protects the drugs from the external environment and prolongs their half-life, it can also be designed to release the cargo in a controlled way and on demand (at required specific conditions). One of the most exciting characteristics of the $CaCO_3$ crystals is their sensitivity to different pH values which allows the cargo to be released in specific sites or conditions. Min K. and co-workers [128] published a detailed work where pH sensitivity was used for the smart release of antibiotics. This is a fascinating topic and despite the significant advances that have been demonstrated, there is still work to be done to tune the pH sensitivity in a way that the cargo is released at a specific and narrow pH range. One possible solution to overcome this is the association of the $CaCO_3$ crystals with additives that can mediate the solubility of the crystals.

$CaCO_3$ presents three anhydrous polymorphs (calcite, vaterite and aragonite) which have been applied as carriers for antimicrobials with very attractive results. Interestingly, despite vaterite being one of the most attractive carriers for drugs, the works reporting the use of $CaCO_3$ as antimicrobial carriers do not show a preference for this polymorph (Tables 1–5). While in some works the use of a polymorph type is deliberated, in other reports it is unclear why a certain polymorph or a mixture of polymorphs is chosen. It would be attractive to use vaterite in more scientific works due to its unique features. Research work where the three polymorphs are compared as carriers for the same drug at similar experimental conditions would also be desirable.

Another topic not systematically studied yet is the effect of $CaCO_3$ crystal sizes on the antimicrobial activity. Carriers size is a crucial characteristic as it affects the interactions with the microorganisms and the ability to cross the cell membranes. There are various works where $CaCO_3$ crystals with micro- and nano-sizes are used for antimicrobials delivery but there aren't reports where the comparison of crystals with different sizes is done. Studies on this topic would allow to optimize the therapeutic effect of $CaCO_3$ crystals as antimicrobials carriers.

Finally, some critically ill patients require the use of different antimicrobial agents concomitantly [154,155]. All the research work discussed in this review used $CaCO_3$ carriers for the transportation of a single therapeutic agent, with the exception of Islan G. et al. [118] report, who associated an antibiotic (levofloxacin) with a mucolytic agent (DNase). It would be of interest to study the advantages of combining different therapeutic agents in the same carrier and ultimately to develop vectors able to increase the therapeutic effect. Such works may appear in nearest future and this review can stimulate the progress towards this direction.

5. Conclusion

$CaCO_3$ crystals present an enormous potential as carriers for antimicrobials. Crystal synthesis allows the fabrication of particles with different sizes, morphologies, surface area and physical-chemical properties using different adjustable affecters such as pH, temperature, reagents ratios and additives. The capacity to host and protect high amounts of various antimicrobials and to deliver them in a controlled, and in some cases, in a stimuli-response fashion proves the versatility of the crystals as modern and advanced drug delivery systems. Several works have explored the use of $CaCO_3$ as carriers for delivery of antimicrobial agents with studies demonstrating a pH-dependent controlled release without affecting the antimicrobial activity and, in some cases, even improving it. The use of $CaCO_3$ as carriers for multiple drugs opens new avenues for combating multidrug resistance which nowadays is one of the major obstacles for successful antimicrobial therapies. The different approaches reported so far for loading $CaCO_3$ particles with antimicrobials demonstrates their high versatility, with the synthesis variations being almost endless. Moreover, the simple synthesis methods and affordable reagents, makes them highly attractive when compared with carriers that require long, complex and expensive fabrication methods. The good biocompatibility results anticipate their safety in humans, a determinant factor for their introduction in the market as drug delivery systems. In this context, more efforts on the evaluation of the cytotoxicity, pharmacokinetics and possible side effects of $CaCO_3$-based delivery vectors are expected in the nearest future. Although the research on this topic is still relatively new, and has only

reached the pre-clinical stage, current usage of $CaCO_3$ as a food supplement and as an pharmaceutical additive approved by the FDA might significantly accelerate its further approval for drug delivery and smooth the bench-to-market translation. There is also some work to be done regarding the optimization and programmed release of antimicrobials, which will potentiate the therapeutic effect and increase the scope of applications. This includes improving the pH sensitivity to specific and narrow pH ranges. The study of the effect of the different polymorphs, their size and charge on the transportation, release and antimicrobial activity will also be important to optimize the therapeutic effect. Despite all the challenges reported, the positive results reported so far sign the potential of $CaCO_3$ as extremely attractive and efficient antimicrobial carriers. We strongly believe that research towards $CaCO_3$-based carriers with multiple antimicrobials, and externally triggered or/and programmed release, will fill the gap in the development of antimicrobial delivery systems, and allow to overcome the serious problem of antimicrobial resistance.

Funding

This work was supported by the Marie Skłodowska-Curie PhD Fellowship programme, EC Grant Agreement No: 801604-DTA3-H2020-MSCA-COFUND-2017. A.V. acknowledges the European Union's Horizon 2020 research and innovation programme (Marie-Curie Individual Fellowship LIGHTOPLEX-747245).

References

[1] World Health Organization, Global Action Plan on Antimicrobial Resistance, Geneva, Switzerland (2015), https://doi.org/10.1128/microbe.10.354.1.
[2] CDC, Antibiotic Resistance Threats in the United States 2019, Atlanta, GA: U.S (2019), https://doi.org/10.15620/cdc:82532.
[3] Public Health England, Health Matters: Antimicrobial Resistance, https://www.gov.uk/government/publications/health-matters-antimicrobial-resistance/health-matters-antimicrobial-resistance, (2015) (accessed March 27, 2020).
[4] L. Rizzello, P.P. Pompa, Nanosilver-based antibacterial drugs and devices: mechanisms, methodological drawbacks, and guidelines, Chem. Soc. Rev. 43 (2014) 1501–1518, https://doi.org/10.1039/c3cs60218d.
[5] D.H. Deck, L.G. Winston, Chemotherapeutic drugs, in: B. Katzung, A. Trevor (Eds.), Basic Clinical. Pharmacology, 13th ed., McGraw-Hill Education, San Francisco, 2015, pp. 1126–1214.
[6] G.H. Talbot, A. Jezek, B.E. Murray, R.N. Jones, R.H. Ebright, G.J. Nau, K.A. Rodvold, J.G. Newland, H.W. Boucher, The infectious diseases society of America's 10 × '20 initiative (10 new systemic antibacterial agents US food and drug administration approved by 2020): is 20 × 20 a possibility? Clin. Infect. Dis. 69 (2019) 1–11, https://doi.org/10.1093/cid/ciz089.
[7] R.Y. Pelgrift, A.J. Friedman, Nanotechnology as a therapeutic tool to combat microbial resistance ☆, Adv. Drug Deliv. Rev. 65 (2013) 1803–1815, https://doi.org/10.1016/j.addr.2013.07.011.
[8] S. Kumar, S. Bandyopadhyay, P. Das, I. Samanta, P. Mukherjee, S. Roy, B. Kundu, Understanding osteomyelitis and its treatment through local drug delivery system, Biotechnol. Adv. 34 (2016) 1305–1317, https://doi.org/10.1016/j.biotechadv.2016.09.005.
[9] S. Maleki Dizaj, F. Lotfipour, M. Barzegar-Jalali, M.H. Zarrintan, K. Adibkia, Ciprofloxacin HCl-loaded calcium carbonate nanoparticles: preparation, solid state characterization, and evaluation of antimicrobial effect against *Staphylococcus aureus*, Artif. Cells, Nanomed. Biotechnol. 45 (2017) 535–543, https://doi.org/10.3109/21691401.2016.1161637.
[10] N. Kavanagh, E.J. Ryan, A. Widaa, G. Sexton, J. Fennell, S. O'Rourke, K.C. Cahill, C.J. Kearney, F.J. O'Brien, S.W. Kerrigana, Staphylococcal osteomyelitis: disease progression, treatment challenges, and future directions, Clin. Microbiol. Rev. 31 (2018) 1–25, https://doi.org/10.1128/CMR.00084-17.
[11] S. Maleki Dizaj, F. Lotfipour, M. Barzegar-Jalali, M.H. Zarrintan, K. Adibkia, Physicochemical characterization and antimicrobial evaluation of gentamicin-loaded CaCO3 nanoparticles prepared via microemulsion method, J. Drug Deliv. Sci. Technol. 35 (2016) 16–23, https://doi.org/10.1016/j.jddst.2016.05.004.
[12] R. Nordström, M. Malmsten, Delivery systems for antimicrobial peptides, Adv. Colloid Interf. Sci. 242 (2017) 17–34, https://doi.org/10.1016/j.cis.2017.01.005.
[13] A. Gupta, S. Mumtaz, C.-H. Li, I. Hussain, V.M. Rotello, Combatting antibiotic-resistant bacteria using nanomaterials, Chem. Soc. Rev. 48 (2019) 415–427.
[14] B. Singh, J. Na, M. Konarova, T. Wakihara, Y. Yamauchi, C. Salomon, M.B. Gawande, Functional mesoporous silica nanoparticles for catalysis and environmental applications, Bull. Chem. Soc. Jpn. (2020), https://doi.org/10.1246/bcsj.20200136.
[15] A. Gonzalez Gomez, Z. Hosseinidoust, Liposomes for antibiotic encapsulation and delivery, ACS Infect. Dis. 6 (2020) 896–908, https://doi.org/10.1021/acsinfecdis.9b00357.
[16] A. Simonazzi, A.G. Cid, M. Villegas, A.I. Romero, S.D. Palma, J.M. Bermúdez, Nanotechnology applications in drug controlled release, Drug Targeting and Stimuli Sensitive Drug Delivery System, 2018, https://doi.org/10.1016/b978-0-12-813689-8.00003-3.
[17] I. Negut, V. Grumezescu, G. Dorcioman, G. Socol, Microscale drug delivery systems: current perspectives and novel approaches, Nano- Microscale Drug Delivery System Design and Fabrication, 2017, https://doi.org/10.1016/B978-0-323-52727-9.00001-7.
[18] A.C. Anselmo, S. Mitragotri, An overview of clinical and commercial impact of drug delivery systems, J. Control. Release (2014), https://doi.org/10.1016/j.jconrel.2014.03.053.
[19] J. Siepmann, F. Siepmann, Microparticles used as drug delivery systems, Progr. Colloid Polym. Sci. 133 (2006) 15–21, https://doi.org/10.1007/2882_053.
[20] A.M. Pisoschi, A. Pop, C. Cimpeanu, V. Turcuș, G. Predoi, F. Iordache, Nanoencapsulation techniques for compounds and products with antioxidant and antimicrobial activity - a critical view, Eur. J. Med. Chem. 157 (2018) 1326–1345, https://doi.org/10.1016/j.ejmech.2018.08.076.
[21] D.B. Trushina, T.V. Bukreeva, M.V. Kovalchuk, M.N. Antipina, CaCO3 vaterite microparticles for biomedical and personal care applications, Mater. Sci. Eng. C 45 (2014) 644–658, https://doi.org/10.1016/j.msec.2014.04.050.
[22] Y. Boyjoo, V.K. Pareek, J. Liu, Synthesis of micro and nano-sized calcium carbonate particles and their applications, J. Mater. Chem. A 2 (2014) 14270–14288, https://doi.org/10.1039/c4ta02070g.
[23] M. Brito, E. Case, W.M. Kriven, A. Zhu, Tas, use of vaterite and calcite in forming calcium phosphate cement scaffolds. Developments in porous, biological and geopolymer ceramics, Eng. Sci. Proc. 28 (2008) 135–150.
[24] J. Vuola, H. Göransson, T. Böhling, S. Asko-Seljavaara, Bone marrow induced osteogenesis in hydroxyapatite and calcium carbonate implants, Biomaterials. 17 (1996) 1761–1766, https://doi.org/10.1016/0142-9612(95)00351-7.
[25] N. Feoktistova, J. Rose, V.Z. Prokopović, A.S. Vikulina, A. Skirtach, D. Volodkin, Controlling the vaterite CaCO3 crystal pores. Design of tailor-made polymer based microcapsules by hard templating, Langmuir 32 (2016) 4229–4238, https://doi.org/10.1021/acs.langmuir.6b00717.
[26] G. Begum, T.N. Reddy, K.P. Kumar, K. Dhevendar, S. Singh, M. Amarnath, S. Misra, V.K. Rangari, R.K. Rana, In situ strategy to encapsulate antibiotics in a bioinspired CaCO 3 structure enabling pH-sensitive drug release apt for therapeutic and imaging applications, ACS Appl. Mater. Interfaces 8 (2016) 22056–22063, https://doi.org/10.1021/acsami.6b07177.
[27] S.V. German, M.V. Novoselova, D.N. Bratashov, P.A. Demina, V.S. Atkin, D.V. Voronin, B.N. Khlebtsov, B.V. Parakhonskiy, G.B. Sukhorukov, D.A. Gorin, High-efficiency freezing-induced loading of inorganic nanoparticles and proteins into micron- and submicron-sized porous particles, Sci. Rep. 8 (2018) 1–10, https://doi.org/10.1038/s41598-018-35846-x.
[28] EFSA, Scientific opinion on re-evaluation of calcium carbonate (E 170) as a food additive, EFSA J. 9 (2011) 1–73, https://doi.org/10.2903/j.efsa.2011.2318.
[29] M. Maleki Dizaj, M. Barzegar-Jalali, M.H. Zarrintan, K. Adibkia, F. Lotfipour, Calcium carbonate nanoparticles as cancer drug delivery system, Expert Opin. Drug Deliv. 12 (2015) 1649–1660, https://doi.org/10.1517/17425247.2015.1049530.
[30] S. Haruta, T. Hanafusa, H. Fukase, H. Miyajima, T. Oki, An effective absorption behavior of insulin for diabetic, Diabetes Thechnol. Ther. 5 (2003) 1–9.
[31] D. Green, D. Walsh, X. Yang, R.O.C. Oreffo, Stimulation of human bone marrow stromal cells using growth factor encapsulated calcium carbonate porous microspheres, J. Mater. Chem. 14 (2004) 2206–2212.
[32] X. He, T. Liu, Y. Chen, D. Cheng, X. Li, Y. Xiao, Y. Feng, Calcium carbonate nanoparticle delivering vascular endothelial growth factor-C siRNA effectively inhibits lymphangiogenesis and growth of gastric cancer in vivo, Cancer Gene Ther. 15 (2008) 193–202, https://doi.org/10.1038/sj.cgt.7701122.
[33] S. Chen, F. Li, R. Zhuo, S. Cheng, Molecular BioSystems Efficient non-viral gene delivery mediated by nanostructured calcium carbonate in solution-based transfection and solid-phase transfection, Mol. BioSyst. 7 (2011) 2841–2847, https://doi.org/10.1039/c1mb05147d.
[34] N.G. Balabushevich, A.V. Lopez De Guerenu, N.A. Feoktistova, D. Volodkin, Protein loading into porous CaCO3 microspheres: adsorption equilibrium and bioactivity retention, Phys. Chem. Chem. Phys. 17 (2015) 2523–2530, https://doi.org/10.1039/c4cp04567j.
[35] A.S. Vikulina, N.A. Feoktistova, N.G. Balabushevich, A.G. Skirtach, D. Volodkin, The mechanism of catalase loading into porous vaterite CaCO3 crystals by co-synthesis, Phys. Chem. Chem. Phys. 20 (2018) 8822–8831, https://doi.org/10.1039/c7cp07836f.
[36] P.V. Binevski, N.G. Balabushevich, V.I. Uvarova, A.S. Vikulina, D. Volodkin, Biofriendly encapsulation of superoxide dismutase into vaterite CaCO3 crystals. Enzyme activity, release mechanism, and perspectives for ophthalmology, Colloids Surf. B: Biointerfaces 181 (2019) 437–449, https://doi.org/10.1016/j.colsurfb.2019.05.077.
[37] T. Yang, Z. Wan, Z. Liu, H. Li, H. Wang, N. Lu, Z. Chen, X. Mei, X. Ren, In situ mineralization of anticancer drug into calcium carbonate monodisperse nanospheres and their pH-responsive release property, Mater. Sci. Eng. C 63 (2016) 384–392, https://doi.org/10.1016/j.msec.2016.03.009.
[38] S.A. Kamba, M. Ismail, S.H. Hussein-al-ali, T. Azmi, T. Ibrahim, Z. Abu, B. Zakaria, In Vitro Delivery and Controlled Release of Doxorubicin for Targeting Osteosarcoma Bone Cancer, (2013), pp. 10580–10598, https://doi.org/10.3390/molecules180910580.
[39] X. Ma, L. Li, L. Yang, C. Su, Y. Guo, K. Jiang, Preparation of highly ordered hierarchical CaCO 3 hemisphere and the application as pH value-sensitive anticancer drug carrier, Mater. Lett. 65 (2011) 3176–3179, https://doi.org/10.1016/j.

matlet.2011.07.009.
[40] V.E. Bosio, M.L. Cacicedo, B. Calvignac, I. León, T. Beuvier, F. Boury, G.R. Castro, Colloids and surfaces B : biointerfaces synthesis and characterization of CaCO 3 – biopolymer hybrid nanoporous microparticles for controlled release of doxorubicin, Colloids Surf. B: Biointerfaces 123 (2014) 158–169, https://doi.org/10.1016/j.colsurfb.2014.09.011.
[41] Y. Ueno, H. Futagawa, Y. Takagi, A. Ueno, Y. Mizushima, Drug-incorporating calcium carbonate nanoparticles for a new delivery system, 103 (2005), pp. 93–98, https://doi.org/10.1016/j.jconrel.2004.11.015.
[42] R. Beck, J.P. Andreassen, The onset of spherulitic growth in crystallization of calcium carbonate, J. Cryst. Growth 312 (2010) 2226–2238, https://doi.org/10.1016/j.jcrysgro.2010.04.037.
[43] Y.G. Bushuev, A.R. Finney, P.M. Rodger, Stability and structure of hydrated amorphous calcium carbonate, Cryst. Growth Des. 15 (2015) 5269–5279, https://doi.org/10.1021/acs.cgd.5b00771.
[44] A.M. Chaka, Ab initio thermodynamics of hydrated calcium carbonates and calcium analogues of magnesium carbonates: implications for carbonate crystallization pathways, ACS Earth Sp. Chem. 2 (2018) 210–224, https://doi.org/10.1021/acsearthspacechem.7b00101.
[45] K.K. Sand, J.D. Rodriguez-Blanco, E. Makovicky, L.G. Benning, S.L.S. Stipp, Crystallization of CaCO 3 in water-alcohol mixtures: spherulitic growth, polymorph stabilization, and morphology change, Cryst. Growth Des. 12 (2012) 842–853, https://doi.org/10.1021/cg2012342.
[46] A. Lucas, J. Gaudé, C. Carel, J.F. Michel, G. Cathelineau, A synthetic aragonite-based ceramic as a bone graft substitute and substrate for antibiotics, Int. J. Inorg. Mater. 3 (2001) 87–94, https://doi.org/10.1016/S1466-6049(00)00058-1.
[47] D.V. Volodkin, N.I. Larionova, G.B. Sukhorukov, Protein encapsulation via porous CaCO3 microparticles templating, Biomacromolecules. 5 (2004) 1962–1972, https://doi.org/10.1021/bm049669e.
[48] D. Konopacka-Łyskawa, Synthesis methods and favorable conditions for spherical vaterite precipitation: A review, Crystals 9 (2019), https://doi.org/10.3390/cryst9040223.
[49] A. Sergeeva, R. Sergeev, E. Lengert, A. Zakharevich, B. Parakhonskiy, D. Gorin, S. Sergeev, D. Volodkin, Composite magnetite and protein containing CaCO3 crystals. External manipulation and vaterite → calcite recrystallization-mediated release performance, ACS Appl. Mater. Interfaces 7 (2015) 21315–21325, https://doi.org/10.1021/acsami.5b05848.
[50] D. Volodkin, CaCO3 templated micro-beads and -capsules for bioapplications, Adv. Colloid Interf. Sci. 207 (2014) 306–324, https://doi.org/10.1016/j.cis.2014.04.001.
[51] G. Wu, Y. Wang, S. Zhu, J. Wang, Preparation of ultrafine calcium carbonate particles with micropore dispersion method, Powder Technol. (2007), https://doi.org/10.1016/j.powtec.2006.10.031.
[52] C. Wang, Y. Sheng, X. Zhao, Y. Pan, Hari-Bala, Z. Wang, Synthesis of hydrophobic CaCO3 nanoparticles, Mater. Lett. (2006), https://doi.org/10.1016/j.matlet.2005.10.035.
[53] Y. Wen, L. Xiang, Y. Jin, Synthesis of plate-like calcium carbonate via carbonation route, Mater. Lett. 57 (2003) 2565–2571, https://doi.org/10.1016/S0167-577X(02)01312-5.
[54] S. Houngaloune, K.S. Ariffin, H. Bin Hussin, K. Watanabe, V. Nhinxay, The effects of limestone characteristic, granulation and calcination temperature to the reactivity of quicklime, Malaysian J. Microsc. 6 (2010) 53–57.
[55] L. Xiang, Y. Wen, Q. Wang, Y. Jin, Formation and characterization of dispersive Mg substituted CaCO 3, Mater. Lett. (2006), https://doi.org/10.1016/j.matlet.2005.12.008.
[56] W. Chuajiw, K. Takatori, T. Igarashi, H. Hara, Y. Fukushima, The influence of aliphatic amines, diamines, and amino acids on the polymorph of calcium carbonate precipitated by the introduction of carbon dioxide gas into calcium hydroxide aqueous suspensions, J. Cryst. Growth (2014), https://doi.org/10.1016/j.jcrysgro.2013.10.009.
[57] L.B. Gower, D.J. Odom, Deposition of calcium carbonate films by a polymer-induced liquid-precursor (PILP) process, J. Cryst. Growth 210 (2000) 719–734.
[58] M. Faatz, F. Gröhn, G. Wegner, Mineralization of calcium carbonate by controlled release of carbonate in aqueous solution, Mater. Sci. Eng. C (2005), https://doi.org/10.1016/j.msec.2005.01.005.
[59] C.K. Ahn, H.W. Lee, M.W. Lee, Y.S. Chang, K. Han, C.H. Rhee, J.Y. Kim, H.D. Chun, J.M. Park, Determination of ammonium salt/ion speciation in the CO2 absorption process using ammonia solution: modeling and experimental approaches, Energy Procedia 4 (2011) 541–547, https://doi.org/10.1016/j.egypro.2011.01.086.
[60] H.S. Liu, K.A. Chen, C.Y. Tai, Droplet stability and product quality in the Higee-assisted microemulsion process for preparing CaCO3 particles, Chem. Eng. J. (2012), https://doi.org/10.1016/j.cej.2012.05.022.
[61] D.B. Trushina, T.V. Bukreeva, M.N. Antipina, Size-controlled synthesis of vaterite calcium carbonate by the mixing method: aiming for Nanosized particles, Cryst. Growth Des. 16 (2016) 1311–1319, https://doi.org/10.1021/acs.cgd.5b01422.
[62] Ç.M. Oral, B. Ercan, Influence of pH on morphology, size and polymorph of room temperature synthesized calcium carbonate particles, Powder Technol. 339 (2018) 781–788, https://doi.org/10.1016/j.powtec.2018.08.066.
[63] C.Y. Tai, F. Chen, Polymorphism of CaCO3, Precipitated in a Contant-Composition Environment, AIChE 44 (1998) 1790–1798, https://doi.org/10.1002/aic.690440810.
[64] Y. Sheng Han, G. Hadiko, M. Fuji, M. Takahashi, Crystallization and transformation of vaterite at controlled pH, J. Cryst. Growth (2006), https://doi.org/10.1016/j.jcrysgro.2005.11.011.
[65] M. Ma, Y. Wang, X. Cao, W. Lu, Y. Guo, Temperature and supersaturation as key parameters controlling the spontaneous precipitation of calcium carbonate with distinct physicochemical properties from pure aqueous solutions, Cryst. Growth Des. 19 (2019) 6972–6988, https://doi.org/10.1021/acs.cgd.9b00758.
[66] T. Ogino, T. Suzuki, K. Sawada, The formation and transformation mechanism of calcium carbonate in water, Geochim. Cosmochim. Acta 51 (1987) 2757–2767, https://doi.org/10.1016/0016-7037(87)90155-4.
[67] J. Chen, L. Xiang, Controllable synthesis of calcium carbonate polymorphs at different temperatures, Powder Technol. (2009), https://doi.org/10.1016/j.powtec.2008.06.004.
[68] R. Ševčík, M. Pérez-Estébanez, A. Viani, P. Šašek, P. Mácová, Characterization of vaterite synthesized at various temperatures and stirring velocities without use of additives, Powder Technol. (2015), https://doi.org/10.1016/j.powtec.2015.06.064.
[69] N. Spanos, P.G. Koutsoukos, Kinetics of precipitation of calcium carbonate in alkaline pH at constant supersaturation. Spontaneous and seeded growth, J. Phys. Chem. B 102 (1998) 6679–6684, https://doi.org/10.1021/jp981171h.
[70] M. Kitamura, Strategy for control of crystallization of polymorphs, CrystEngComm. 11 (2009) 949–964, https://doi.org/10.1039/b809332f.
[71] C.Y. Tai, P. Chen, Morphology of calcium carbonate, AIChE. 41 (1995) 68–77.
[72] B. Njegić-Džakula, G. Falini, L. Brečević, Ž. Skoko, D. Kralj, Effects of initial supersaturation on spontaneous precipitation of calcium carbonate in the presence of charged poly-l-amino acids, J. Colloid Interface Sci. (2010), https://doi.org/10.1016/j.jcis.2009.12.010.
[73] H. Bahrom, A.A. Goncharenko, L.I. Fatkhutdinova, O.O. Peltek, A.R. Muslimov, O.Y. Koval, I.E. Eliseev, A. Manchev, D. Gorin, I.I. Shishkin, R.E. Noskov, A.S. Timin, P. Ginzburg, M.V. Zyuzin, Controllable synthesis of calcium carbonate with different geometry: comprehensive analysis of particle formation, cellular uptake, and biocompatibility, ACS Sustain. Chem. Eng. 7 (2019), https://doi.org/10.1021/acssuschemeng.9b05128 acssuschemeng.9b05128.
[74] D.V. Volodkin, S. Schmidt, P. Fernandes, N.I. Larionova, G.B. Sukhorukov, C. Duschl, H. Möhwald, R. Von Klitzing, One-step formulation of protein microparticles with tailored properties: hard templating at soft conditions, Adv. Funct. Mater. 22 (2012) 1914–1922, https://doi.org/10.1002/adfm.201103007.
[75] S. Maleki Dizaj, F. Lotfipour, M. Barzegar-Jalali, M.H. Zarrintan, K. Adibkia, Application of Box–Behnken design to prepare gentamicin-loaded calcium carbonate nanoparticles, Artif. Cells, Nanomed. Biotechnol. 44 (2016) 1475–1481, https://doi.org/10.3109/21691401.2015.1042108.
[76] Y. Mori, T. Enomae, A. Isogai, Preparation of pure vaterite by simple mechanical mixing of two aqueous salt solutions, Mater. Sci. Eng. C 29 (2009) 1409–1414, https://doi.org/10.1016/j.msec.2008.11.009.
[77] Y. Wang, Y.X. Moo, C. Chen, P. Gunawan, R. Xu, Fast precipitation of uniform CaCO3 nanospheres and their transformation to hollow hydroxyapatite nanospheres, J. Colloid Interface Sci. 352 (2010) 393–400, https://doi.org/10.1016/j.jcis.2010.08.060.
[78] M.L.P. Vidallon, F. Yu, B.M. Teo, Controlling size and polymorphism of calcium carbonate hybrid particles using natural biopolymers, Cryst. Growth Des. 20 (2020) 645–652, https://doi.org/10.1021/acs.cgd.9b01057.
[79] B.V. Parakhonskiy, A. Haase, R. Antolini, Sub-micrometer vaterite containers: synthesis, substance loading, and release, Angew. Chem. Int. Ed. 51 (2012) 1195–1197, https://doi.org/10.1002/anie.201104316.
[80] F. Manoli, E. Dalas, Spontaneous precipitation of calcium carbonate in the presence of ethanol, isopropanol and diethylene glycol, J. Cryst. Growth 218 (2000) 359–364, https://doi.org/10.1016/S0022-0248(00)00560-1.
[81] X.-H. Guo, S.-H. Yu, G.-B. Cai, Crystallization in a mixture of solvents by using a crystal modifier: morphology control in the synthesis of highly monodisperse CaCO3 microspheres, Angew. Chem. 118 (2006) 4081–4085, https://doi.org/10.1002/ange.200600029.
[82] D. Gebauer, H. Cölfen, A. Verch, M. Antonietti, The multiple roles of additives in CaCO3 crystallization: a quantitative case study, Adv. Mater. 21 (2009) 435–439, https://doi.org/10.1002/adma.200801614.
[83] R.-Q. Song, H. Colfen, Additive controlled crystallization, Crystengcomm. 13 (2011) 1249–1276, https://doi.org/10.1039/c0ce00419g.
[84] G. Begum, R.K. Rana, Bio-inspired motifs via tandem assembly of polypeptides for mineralization of stable CaCO 3 structures, Chem. Commun. 48 (2012) 8216–8218, https://doi.org/10.1039/c2cc32756b.
[85] A.G. Skirtach, A.M. Yashchenok, H. Möhwald, Encapsulation, release and applications of LbL polyelectrolyte multilayer capsules, Chem. Commun. 47 (2011) 12736–12746, https://doi.org/10.1039/c1cc13453a.
[86] A. Vikulina, D. Voronin, D. Voronin, R. Fakhrullin, V. Vinokurov, D. Volodkin, Naturally derived nano- and micro-drug delivery vehicles: halloysite, vaterite and nanocellulose, New J. Chem. 44 (2020) 5638–5655, https://doi.org/10.1039/c9nj06470b.
[87] N.A. Feoktistova, N.G. Balabushevich, A.G. Skirtach, D. Volodkin, A.S. Vikulina, Inter-protein interactions govern protein loading into porous vaterite CaCO 3 crystals, Phys. Chem. Chem. Phys. 22 (2020) 9713–9722, https://doi.org/10.1039/d0cp00404a.
[88] S. Schmidt, M. Behra, K. Uhlig, N. Madaboosi, L. Hartmann, C. Duschl, D. Volodkin, Mesoporous protein particles through colloidal CaCO3 templates, Adv. Funct. Mater. 23 (2013) 116–123, https://doi.org/10.1002/adfm.201201321.
[89] N.G. Balabushevich, A.V. Lopez De Guerenu, N.A. Feoktistova, A.G. Skirtach, D. Volodkin, Protein-containing multilayer capsules by templating on mesoporous CaCO3 particles: POST- and PRE-loading approaches, Macromol. Biosci. 16 (2016) 95–105, https://doi.org/10.1002/mabi.201500243.
[90] A.I. Petrov, D.V. Volodkin, G.B. Sukhorukov, Protein-calcium carbonate coprecipitation: a tool for protein encapsulation, Biotechnol. Prog. 21 (2005) 918–925, https://doi.org/10.1021/bp0495825.

[91] N.A. Feoktistova, A.S. Vikulina, N.G. Balabushevich, A.G. Skirtach, D. Volodkin, Bioactivity of catalase loaded into vaterite CaCO3 crystals via adsorption and co-synthesis, Mater. Des. 185 (2020) 108223, https://doi.org/10.1016/j.matdes.2019.108223.

[92] N.G. Balabushevich, E.A. Kovalenko, I.M. Le-Deygen, L.Y. Filatova, D. Volodkin, A.S. Vikulina, Hybrid CaCO3-mucin crystals: effective approach for loading and controlled release of cationic drugs, Mater. Des. 182 (2019) 108020, https://doi.org/10.1016/j.matdes.2019.108020.

[93] N.G. Balabushevich, E.A. Sholina, E.V. Mikhalchik, L.Y. Filatova, A.S. Vikulina, D. Volodkin, Self-assembled mucin-containing microcarriers via hard templating on CaCO3 crystals, Micromachines. 9 (2018) 1–16, https://doi.org/10.3390/mi9060307.

[94] N.G. Balabushevich, E.A. Kovalenko, E.V. Mikhalchik, L.Y. Filatova, D. Volodkin, A.S. Vikulina, Mucin adsorption on vaterite CaCO 3 microcrystals for the prediction of mucoadhesive properties, J. Colloid Interface Sci. 545 (2019) 330–339, https://doi.org/10.1016/j.jcis.2019.03.042.

[95] B.O. Guillame-gentil, O. Semenov, A.S. Roca, T. Groth, R. Zahn, J. Vörös, M. Zenobi-wong, Engineering the extracellular environment : strategies for building 2D and 3D cellular structures, Adv. Mater. 22 (2010) 5443–5462, https://doi.org/10.1002/adma.201001747.

[96] N. Madaboosi, K. Uhlig, S. Schmidt, A.S. Vikulina, H. Möhwald, C. Duschl, D. Volodkin, A " cell-friendly " window for the interaction of cells with hyaluronic acid/poly- l -lysine multilayers, Macromol. Biosci. 18 (2018) 17003–17019, https://doi.org/10.1002/mabi.201700319.

[97] D. Volodkin, R. Von Klitzing, H. Moehwald, Polyelectrolyte multilayers: towards single cell studies, Polymers (Basel). 6 (2014) 1502–1527, https://doi.org/10.3390/polym6051502.

[98] C. Üzüm, J. Hellwig, N. Madaboosi, D. Volodkin, R. Von Klitzing, Growth behaviour and mechanical properties of PLL/HA multilayer films studied by AFM, Beilstein J. Nanotechnol. 3 (2012) 778–788, https://doi.org/10.3762/bjnano.3.87.

[99] D.G. Shchukin, D.V. Volodkin, Binding mechanism of the model charged dye carboxy fl uorescein to hyaluronan/polylysine multilayers, ACS Appl. Mater. Interfaces 9 (2017) 38908–38918, https://doi.org/10.1021/acsami.7b12449.

[100] N. Velk, K. Uhlig, A. Vikulina, C. Duschl, D. Volodkin, Colloids and surfaces B : biointerfaces mobility of lysozyme in poly (l -lysine)/ hyaluronic acid multilayer films, Colloids Surf. B: Biointerfaces 147 (2016) 343–350, https://doi.org/10.1016/j.colsurfb.2016.07.055.

[101] V.Z. Prokopović, A.S. Vikulina, D. Sustr, C. Duschl, D. Volodkin, Biodegradation-resistant multilayers coated with gold nanoparticles. Toward a tailor-made artificial extracellular matrix, ACS Appl. Mater. Interfaces 8 (2016) 24345–24349, https://doi.org/10.1021/acsami.6b10095.

[102] A.S. Vikulina, Y.G. Anissimov, P. Singh, V.Z. Prokopovic, K. Uhlig, M.S. Jaeger, R. Von Klitzing, C. Duschl, D. Volodkin, Temperature effect on the build-up of exponentially growing polyelectrolyte multilayers. An exponential-to-linear transition point †, Phys. Chem. Chem. Phys. 18 (2016) 9–14, https://doi.org/10.1039/c6cp00345a.

[103] D.V. Volod'kin, N.G. Balabushevitch, G.B. Sukhorukov, N.I. Larionova, Inclusion of proteins into polyelectrolyte microparticles by alternative adsorption of poly-electrolytes on protein aggregates, Biochem. 68 (2003) 283–289.

[104] D.V. Volodkin, N.G. Balabushevitch, G.B. Sukhorukov, N.I. Larionova, Model system for controlled protein release: ph-Sensitive polyelectrolyte microparticles, S.T.P. Pharma Sci. 13 (2003) 163–170.

[105] C.S. Peyratout, L. Dähne, Tailor-made polyelectrolyte microcapsules: from multilayers to smart containers, Angew. Chem. Int. Ed. 43 (2004) 3762–3783, https://doi.org/10.1002/anie.200300568.

[106] L. Jeannot, M. Bell, R. Ashwell, D. Volodkin, A.S. Vikulina, Internal structure of matrix-type multilayer capsules templated on porous vaterite CaCO3 crystals as probed by staining with a fluorescence dye, Micromachines. 9 (2018) 1–15, https://doi.org/10.3390/mi9110547.

[107] A.S. Vikulina, S.T. Aleed, T. Paulraj, Y.A. Vladimirov, C. Duschl, R. Von Klitzing, D. Volodkin, Temperature-induced molecular transport through polymer multilayers coated with PNIPAM, Phys. Chem. Chem. Phys. 17 (2015) 12771–12777, https://doi.org/10.1039/c5cp01213a.

[108] A.S. Vikulina, A.G. Skirtach, D. Volodkin, Hybrids of polymer multilayers, lipids, and nanoparticles: mimicking the cellular microenvironment, Langmuir. 35 (2019) 8565–8573, https://doi.org/10.1021/acs.langmuir.8b04328.

[109] A. Sergeeva, A.S. Vikulina, D. Volodkin, Porous alginate scaffolds assembled using vaterite CaCO3 crystals, Micromachines. 10 (2019) 1–21, https://doi.org/10.3390/mi10060357.

[110] A. Sergeeva, N. Feoktistova, V. Prokopovic, D. Gorin, Design of porous alginate hydrogels by sacrificial CaCO 3 templates : pore formation mechanism, Adv. Mater. Interfaces 2 (2015) 1–10, https://doi.org/10.1002/admi.201500386.

[111] A.S. Sergeeva, D.A. Gorin, D.V. Volodkin, In-situ assembly of Ca − alginate gels with controlled pore loading/release capability, Langmuir 31 (2015), https://doi.org/10.1021/acs.langmuir.5b01529.

[112] T. Paulraj, N. Feoktistova, N. Velk, K. Uhlig, C. Duschl, D. Volodkin, Microporous polymeric 3D scaffolds templated by the layer-by-layer self-assembly, Macromol. Rapid Commun. 35 (2014) 1408–1413.

[113] X. Pan, S. Chen, D. Li, W. Rao, Y. Zheng, Z. Yang, L. Li, X. Guan, Z. Chen, The synergistic antibacterial mechanism of gentamicin-loaded CaCO 3 nanoparticles, Front. Chem. 5 (2018) 1–9, https://doi.org/10.3389/fchem.2017.00130.

[114] P.C. Sahoo, F. Kausar, J.H. Lee, J.I. Han, Facile fabrication of silver nanoparticle embedded CaCO3 microspheres via microalgae-templated CO2 biomineralization: application in antimicrobial paint development, RSC Adv. 4 (2014) 32562–32569, https://doi.org/10.1039/c4ra03623a.

[115] K. Qian, T. Shi, T. Tang, S. Zhang, X. Liu, Y. Cao, Preparation and characterization of nano-sized calcium carbonate as controlled release pesticide carrier for validamycin against Rhizoctonia solani, Microchim. Acta 173 (2011) 51–57, https://doi.org/10.1007/s00604-010-0523-x.

[116] M.Y. Memar, K. Adibkia, S. Farajnia, H.S. Kafil, S. Maleki-Diza, R. Ghotaslou, Biocompatibility, cytotoxicity and antimicrobial effects of gentamicin-loaded CaCO3 as a drug delivery to osteomyelitis, J. Drug Deliv. Sci. Technol. 54 (2019) 101307, https://doi.org/10.1016/j.jddst.2019.101307.

[117] G.A. Islan, M.L. Cacicedo, V.E. Bosio, G.R. Castro, Development and characterization of new enzymatic modified hybrid calcium carbonate microparticles to obtain nano-architectured surfaces for enhanced drug loading, J. Colloid Interface Sci. 439 (2015) 76–87, https://doi.org/10.1016/j.jcis.2014.10.007.

[118] G.A. Islan, M.E. Ruiz, J.F. Morales, M.L. Sbaraglini, A.V. Enrique, G. Burton, A. Talevi, L.E. Bruno-Blanch, G.R. Castro, Hybrid inhalable microparticles for dual controlled release of levofloxacin and DNase: physicochemical characterization and in vivo targeted delivery to the lungs, J. Mater. Chem. B 5 (2017) 3132–3144, https://doi.org/10.1039/c6tb03366k.

[119] A. Lucas-girot, O. Tribut, J. Sangleboeuf, Gentamicin-loaded calcium carbonate materials : comparison of two drug-loading modes, J Biomed Mater Res B Appl Biomater 73 (2005) 164–170, https://doi.org/10.1002/jbm.b.30210.

[120] H. Yang, Y. Wang, T. Liang, Y. Deng, X. Qi, H. Jiang, Y. Wu, H. Gao, Hierarchical porous calcium carbonate microspheres as drug delivery vector, Prog. Nat. Sci. Mater. Int. 27 (2017) 674–677, https://doi.org/10.1016/j.pnsc.2017.11.005.

[121] M. Mihai, S. Racovita, A.L. Vasiliu, F. Doroftei, C. Barbu-Mic, S. Schwarz, C. Steinbach, F. Simon, Autotemplate microcapsules of CaCO3/pectin and non-stoichiometric complexes as sustained tetracycline hydrochloride delivery carriers, ACS Appl. Mater. Interfaces 9 (2017) 37264–37278, https://doi.org/10.1021/acsami.7b09333.

[122] S. Racovita, A.L. Vasiliu, A. Bele, D. Schwarz, C. Steinbach, R. Boldt, S. Schwarz, M. Mihai, Complex calcium carbonate/polymer microparticles as carriers for aminoglycoside antibiotics, RSC Adv. 8 (2018) 23274–23283, https://doi.org/10.1039/c8ra03367f.

[123] F. Ali Said, N. Bousserrhine, V. Alphonse, L. Michely, S. Belbekhouche, Antibiotic loading and development of antibacterial capsules by using porous CaCO3 microparticles as starting material, Int. J. Pharm. 579 (2020) 119175, https://doi.org/10.1016/j.ijpharm.2020.119175.

[124] C. Matei, D. Berger, A. Dumbrava, M.D. Radu, E. Gheorghe, Calcium carbonate as silver carrier in composite materials obtained in green seaweed extract with topical applications, J. Sol-Gel Sci. Technol. (2019), https://doi.org/10.1007/s10971-019-05145-6.

[125] M. Długosz, M. Bulwan, G. Kania, M. Nowakowska, S. Zapotoczny, Hybrid calcium carbonate/polymer microparticles containing silver nanoparticles as antibacterial agents, J. Nanopart. Res. 14 (2012), https://doi.org/10.1007/s11051-012-1313-7.

[126] F. Baldassarre, A. De Stradis, G. Altamura, V. Vergaro, C. Citti, G. Cannazza, A.L. Capodilupo, L. Dini, G. Ciccarella, Application of calcium carbonate nanocarriers for controlled release of phytodrugs against Xylella fastidiosa pathogen, Pure Appl. Chem. (2019) 1–17, https://doi.org/10.1515/pac-2018-1223.

[127] L.D. Tessarolo, R.R.P.P.B. De Menezes, C.P. Mello, D.B. Lima, E.P. Magalhães, E.M. Bezerra, F.A.M. Sales, I.L. Barroso Neto, M.D.F. Oliveira, R.P. Dos Santos, E.L. Albuquerque, V.N. Freire, A.M. Martins, Nanoencapsulation of benznidazole in calcium carbonate increases its selectivity to Trypanosoma cruzi, Parasitology 145 (2018) 1191–1198, https://doi.org/10.1017/S0031182018000197.

[128] K.H. Min, E.Y. Jang, H.J. Lee, Y.S. Hwang, J.I. Ryu, J.H. Moon, S.C. Lee, pH-Responsive mineralized nanoparticles for bacteria-triggered topical release of antibiotics, J. Ind. Eng. Chem. 71 (2019) 210–219, https://doi.org/10.1016/j.jiec.2018.11.027.

[129] J. Xue, X. Li, Q. Li, J. Lyu, W. Wang, L. Zhuang, Y. Xu, Magnetic drug-loaded osteoinductive Fe 3 O 4 /CaCO 3 hybrid microspheres system: efficient for sustained release of antibiotics, J. Phys. D. Appl. Phys. 53 (2020) 245401, https://doi.org/10.1088/1361-6463/ab7bb2.

[130] T. Isa, Z.A.B. Zakaria, Y. Rukayadi, M.N.M. Hezmee, A.Z. Jaji, M.U. Imam, N.I. Hammadi, S.K. Mahmood, Antibacterial activity of ciprofloxacin-encapsulated cockle shells calcium carbonate (Aragonite) nanoparticles and its biocompatability in macrophage J774A.1, Int. J. Mol. Sci. 17 (2016), https://doi.org/10.3390/ijms17050713.

[131] R.V. Padmanabhuni, J. Luo, Z. Cao, Y. Sun, Preparation and characterization of N-halamine-based antimicrobial fillers, Ind. Eng. Chem. Res. 51 (2012) 5148–5156, https://doi.org/10.1021/ie300212x.

[132] V. Apalangya, V. Rangari, B. Tiimob, S. Jeelani, T. Samuel, Development of antimicrobial water filtration hybrid material from bio source calcium carbonate and silver nanoparticles, Appl. Surf. Sci. 295 (2014) 108–114, https://doi.org/10.1016/j.apsusc.2014.01.012.

[133] B.J. Tiimob, G. Mwinyelle, W. Abdela, T. Samuel, S. Jeelani, V.K. Rangari, Nanoengineered eggshell-silver tailored copolyester polymer blend film with antimicrobial properties, J. Agric. Food Chem. 65 (2017) 1967–1976, https://doi.org/10.1021/acs.jafc.7b00133.

[134] C. Ferreira, A.M. Pereira, M.C. Pereira, M. Simões, L.F. Melo, Biofilm control with new microparticles with immobilized biocide, Heat Transf. Eng. 34 (2013) 712–718, https://doi.org/10.1080/01457632.2012.739040.

[135] C. Carel, J. Gaude, A. Lucas, M. Jean-François, Macroporous Composite for Carrying One or More Medicinal Substances and for Use as a Bone Reconstruction Material, and Method for Making Same, EP1019108A1, (1997).

[136] M. Kitamura, H. Konno, A. Yasui, H. Masuoka, Controlling factors and mechanism of reactive crystallization of calcium carbonate polymorphs from calcium hydroxide suspensions, J. Cryst. Growth 236 (2002) 323–332.

[137] Y.I. Svenskaya, H. Fattah, O.A. Inozemtseva, A.G. Ivanova, S.N. Shtykov,

D.A. Gorin, B.V. Parakhonskiy, Key parameters for size- and shape-controlled synthesis of vaterite particles, Cryst. Growth Des. 18 (2018) 331–337, https://doi.org/10.1021/acs.cgd.7b01328.
[138] C. Dhand, M.P. Prabhakaran, R.W. Beuerman, R. Lakshminarayanan, N. Dwivedi, S. Ramakrishna, Role of size of drug delivery carriers for pulmonary and intravenous administration with emphasis on cancer therapeutics and lung-targeted drug delivery, RSC Adv. 4 (2014) 32673–32689, https://doi.org/10.1039/c4ra02861a.
[139] S. Mao, C. Guo, Y. Shi, L.C. Li, Recent advances in polymeric microspheres for parenteral drug delivery - part 1, Expert Opin. Drug Deliv. 9 (2012) 1161–1176, https://doi.org/10.1517/17425247.2012.709844.
[140] R. Ferrari, M. Sponchioni, M. Morbidelli, D. Moscatelli, Polymer nanoparticles for the intravenous delivery of anticancer drugs: the checkpoints on the road from the synthesis to clinical translation, Nanoscale. 10 (2018) 22701–22719, https://doi.org/10.1039/c8nr05933k.
[141] E.J. Begg, M.L. Barclay, C.J.M. Kirkpatrick, The therapeutic monitoring of antimicrobial agents, Br. J. Clin. Pharmacol. 47 (1999) 23–30.
[142] C.L. Ventola, The antibiotic resistance crisis part 1 : causes and threats, P&T. 40 (2015) 277–283.
[143] V.P. Torchilin, Fundamentals of stimuli- responsive drug and gene delivery systems, in: A. Singh, M.M. Amiji (Eds.), Stimuli-Responsive Drug Delivery System, 1st ed., The Royal Society of Chemistry, Croydon, 2018, p. 2.
[144] Z. Dong, L. Feng, W. Zhu, X. Sun, M. Gao, H. Zhao, Y. Chao, Z. Liu, Biomaterials CaCO 3 nanoparticles as an ultra-sensitive tumor-pH-responsive nanoplatform enabling real-time drug release monitoring and cancer combination therapy, Biomaterials. 110 (2016) 60–70, https://doi.org/10.1016/j.biomaterials.2016.09.025.
[145] Z. Wang, X. Zhang, G. Huang, J. Gao, pH-responsive drug delivery systems, in: A. Singh, M.M. Amiji (Eds.), Stimuli-Responsive Drug Delivery System, 1st ed., Royal Society of Chemistry, Croydon, 2018, p. 52.
[146] A.F. Radovic-moreno, T.K. Lu, V.A. Puscasu, C.J. Yoon, R. Langer, O.C. Farokhzad, Surface charge-switching polymeric nanoparticles for bacterial cell wall- targeted delivery of antibiotics, ACS Nano 6 (2012) 4279–4287, https://doi.org/10.1021/nn3008383.
[147] S. Mura, J. Nicolas, P. Couvreur, Stimuli-responsive nanocarriers for drug delivery, Nat. Mater. 12 (2013) 991–1003, https://doi.org/10.1038/nmat3776.
[148] B.V. Parakhonskiy, C. Foss, E. Carletti, M. Fedel, A. Haase, A. Motta, C. Migliaresi, R. Antolini, Tailored intracellular delivery via a crystal phase transition in 400 nm vaterite particles, Biomater. Sci. 1 (2013) 1273–1281, https://doi.org/10.1039/c3bm60141b.
[149] Y.I. Svenskaya, A.M. Pavlov, D.A. Gorin, D.J. Gould, B.V. Parakhonskiy, G.B. Sukhorukov, Photodynamic therapy platform based on localized delivery of photosensitizer by vaterite submicron particles, Colloids Surf. B: Biointerfaces 146 (2016) 171–179, https://doi.org/10.1016/j.colsurfb.2016.05.090.
[150] D.B. Trushina, T.N. Borodina, S.N. Sulyanov, J.V. Moiseeva, N.V. Gulyaeva, T.V. Bukreeva, Comparison of the structural features of micron and submicron vaterite particles and their efficiency for intranasal delivery of Anesthetic to the brain, Crystallogr. Rep. 63 (2018) 998–1004, https://doi.org/10.1134/S1063774518060305.
[151] O. Gusliakova, E.N. Atochina-Vasserman, O. Sindeeva, S. Sindeev, S. Pinyaev, N. Pyataev, V. Revin, G.B. Sukhorukov, D. Gorin, A.J. Gow, Use of submicron vaterite particles serves as an effective delivery vehicle to the respiratory portion of the lung, Front. Pharmacol. 9 (2018) 1–13, https://doi.org/10.3389/fphar.2018.00559.
[152] Y.I. Svenskaya, E.A. Genina, B.V. Parakhonskiy, E.V. Lengert, E.E. Talnikova, G.S. Terentyuk, S.R. Utz, D.A. Gorin, V.V. Tuchin, G.B. Sukhorukov, A simple non-invasive approach toward efficient transdermal drug delivery based on biodegradable particulate system, ACS Appl. Mater. Interfaces 11 (2019) 17270–17282, https://doi.org/10.1021/acsami.9b04305.
[153] A. Som, R. Raliya, L. Tian, W. Akers, J.E. Ippolito, S. Singamaneni, P. Biswas, S. Achilefu, Monodispersed calcium carbonate nanoparticles modulate local pH and inhibit tumor growth: in vivo, Nanoscale. 8 (2016) 12639–12647, https://doi.org/10.1039/c5nr06162h.
[154] S. Kappagoda, U. Singh, B.G. Blackburn, Antiparasitic therapy, Mayo Clin. Proc. 86 (2011) 561–583, https://doi.org/10.4065/mcp.2011.0203.
[155] P.D. Tamma, S.E. Cosgrove, L.L. Maragakis, Combination therapy for treatment of infections with gram-negative bacteria, Clin. Microbiol. Rev. 25 (2012) 450–470, https://doi.org/10.1128/CMR.05041-11.